Acoustic anomalies in terbium molybdate near the improper ferroelastic-ferroelectric phase transition

W. Yao,* H. Z. Cummins, and R. H. Bruce*
Department of Physics, City College - CUNY, New York, New York 10031
(Received 11 September 1980)

The anomaly in the longitudinal elastic constant $\tilde{C}_{11}$ of terbium molybdate (TMO) associated with the ferroelastic-ferroelectric phase transition at 160 °C was investigated by Brillouin scattering spectroscopy. An analysis is presented, based on the phenomenological theory of Levanyuk, which describes both the thermodynamic anomaly due to induced bilinear coupling in the low-symmetry phase and the effects of anharmonic coupling of strain to critical fluctuations of the order parameter which occurs in both phases. Soft-mode dispersion curves from neutron scattering experiments and the temperature-dependent magnitude of the order parameter deduced from x-ray and birefringence studies were used as input for the data-fitting procedures. In our analysis of the data in the low-temperature ferroelectric phase, we consider four models for the second A_1 soft mode which is the partner of the 5.7-meV mode. With the assumption that the coupling constant K_2 between an acoustic phonon and a pair of soft optic phonons is independent of the soft-mode wave vector, only the fourth model produced a self-consistent fit to our data over the range $20\,°C \leq T \leq 400\,°C$ which is also consistent with previous studies of the soft mode.

I. INTRODUCTION

Soft optical modes whose condensation results in structural phase transitions and spontaneous symmetry breaking have been widely investigated by inelastic neutron scattering and Raman scattering experiments.[1,2] Such transitions have also been studied extensively through the temperature-dependent elastic properties resulting from interaction of the soft optical mode with acoustic modes, employing ultrasonic, acoustic resonance, and Brillouin scattering techniques.

The nature of the acoustic anomalies associated with structural phase transitions can be separated into two principal categories depending on the form of the leading interaction term permitted by crystal symmetry in the Landau free energy.[3,4]

If ϵ and η represent the strain and the soft-mode amplitude (or order parameter), respectively, then category (1) includes all crystals for which bilinear interaction terms of the form $a\epsilon\eta$ are symmetry allowed. For these crystals (e.g., potassium dihydrogen phosphate),[5,6] the soft mode must be at the center of the Brillouin zone in both phases, and it is also Raman active in both phases. The Raman-activity criterion, first noted by Miller and Axe,[7] follows from the Worlock-Birman theorem ("the soft mode is always Raman active in the ordered phase"[8]) together with the observation that bilinear coupling in the high-symmetry phase is forbidden unless the order parameter η transforms under the crystal point group as some component of a symmetric second-rank tensor—the strain, or equivalently, the dielectric tensor—which is also the standard requirement for Raman activity. This category automatically includes piezoelectric ferroelectrics since piezoelectricity in the high-symmetry phase requires that the soft mode have the same symmetry as a strain, as well as that it be dipole active.

The acoustic anomalies observed in category (1) crystals are very pronounced since the bilinear interaction hybridizes the soft mode with the acoustic mode to which it couples. Near the transition, the mostly-acoustic hybrid mode frequency (ω_-) drops sharply, actually reaching zero at the transition temperature if the transition is second order. The anomalous sound velocity or Brillouin shift observed in these crystals can usually be explained by a simple thermodynamic analysis based on the Landau free energy.[9]

Category (2), with which we will be primarily concerned, consists of crystals in which bilinear coupling is forbidden by symmetry either because the soft mode does not transform according to the same representation as any strain (e.g., quartz[10] or triglycine sulfate[11]) or because the soft mode in the high-symmetry prototype phase is at an edge or corner of the Brillouin zone rather than at the zone center (e.g., the perovskites[12–14] or the rare-earth molybdates[15]). The lowest-order coupling permitted by symmetry is then a third-order nonlinear interaction, involving terms in the free energy of the form $K\epsilon\eta$.[2] The elastic anomaly which results consists of two distinct effects.[13]

First, there is a morphically induced effective bilinear coupling in the low-symmetry phase resulting from the finite expectation value of the order parameter $\langle \eta \rangle = \eta_0$. Again, a simple thermodynamic analysis shows that while the elastic constant above the transition is unaffected by the coupling, there is a discontinuous downward displacement of the elastic constant below the transition.[9] In ferroelectrics, this produces a temperature-dependent morphic piezoelectric effect which disappears at (and above) the transition.

Additionally, however, the third-order nonlinear interaction can become important close to the transition when the critical fluctuations in η become large, leading to a downward bending of the elastic constant on both sides of the transition.

Miller and Axe[7] and Axe and Shirane[10] have discussed the downward bending of the elastic constants of quartz in the high-temperature β phase in terms of critical fluctuations. (Since the soft mode is Raman inactive in the high-temperature β phase, no bilinear interactions exist.) Barrett analyzed the temperature-dependent ultrasonic attenuation and velocity in $KTaO_3$ in terms of a similar coupling formulated, however, in terms of an Akhieser interaction.[13]

Nonlinear interactions between acoustic and soft optic modes in $SrTiO_3$ and $BaTiO_3$ have been investigated extensively by many workers. Fleury and Lazay,[16] Bell and Ruprecht,[17] and Golding[18] measured the temperature-dependent elastic constants; Dvorak[19] and Slonczewski and Thomas[12] considered the theory of effective bilinear mode interaction in the low-symmetry phase, while Pytte[20] and Pytte and Feder[21] explored the effects of critical fluctuations on the acoustic modes.

In these investigations of crystals where bilinear coupling is forbidden, including studies of the rare-earth molybdates which we will discuss in Sec. II, the two contributions to the elastic anomaly are normally analyzed individually. The induced bilinear coupling in the low-symmetry phase is analyzed either with thermodynamics or, equivalently, with linearized equations of motion, while the critical fluctuation effects are usually analyzed with arguments using thermodynamic Green's functions. Each calculation leads to predictions for the appropriate contribution to the acoustic anomaly whose form can be compared with the results of experiments. Both contain unknown (and apparently unrelated) anharmonic coupling constants whose values are presumably to be found from data fitting.

An alternative approach to the analysis of third-order acoustic-soft–optic-mode interactions was discussed by Levanyuk in 1966.[22] Classical continuum equations of motion are derived from the Landau free energy, but both first- *and second*-order small terms are retained. The fluctuation dissipation theorem is then employed to evaluate the fluctuation terms, and expressions are obtained for the elastic constants which include both the thermodynamic (effective bilinear) and the critical fluctuation contributions to the elastic anomaly. The critical fluctuation contribution is identical to the result of thermodynamic Green's-function analysis, representing virtual intermediate states in which an acoustic phonon has been annihilated, creating a pair of soft optic phonons with equal and opposite momenta. (This is the lowest-order contribution to the anharmonic self-energy of acoustic phonons.) Levanyuk's approach allows the data analysis to be performed self-consistently since the same coupling constants appear in both the thermodynamic and critical fluctuation contributions to the elastic anomaly.

In this paper we report the results of a Brillouin scattering investigation of terbium molybdate (TMO) for which extensive information on the soft-mode characteristics is available from the neutron scattering investigations of Dorner, Axe, and Shirane.[23,24] In Sec. II we summarize the properties of and previous investigations of the rare-earth molybdates. In Sec. III we review Levanyuk's approach and derive the fundamental expressions for the elastic anomalies. In Sec. IV we describe the experiments, and in Sec. V we analyze our experimental results using the equations derived in Sec. III. We investigate four models of the soft mode in the low-symmetry phase and show that a self-consistent interpretation of the observed elastic anomalies can be obtained only if certain as yet untested aspects of the soft mode are assumed to hold.

II. RARE-EARTH MOLYBDATES

The rare-earth molybdates $Gd_2(MoO_4)_3$ (abbreviated as GMO) and its Sm, Eu, Tb, and Dy isomorphs were first shown to be ferroelectric, with transition temperatures T_0 near 160 °C, by Borchardt and Bierstedt in 1966.[25,26] Cross, Fouskova, and Cummins investigated the electrical, optical, and mechanical behavior of GMO and discovered a number of unusual characteristics.[27–29] The low-temperature phase is both ferroelectric and ferroelastic. The coupled polarization and shear strain switch simultaneously under either applied stress or electric field. There is a very small dielectric anomaly at T_0 which disappears entirely for the inertially clamped crystal. These observations led Cross *et al.* to propose that the essential instability driving the transition is elastic, with spontaneous polarization arising as a secondary consequence of piezoelectric coupling, but this explanation of improper ferroelectricity in GMO conflicted with the marked asymmetry in the elastic anomaly which they observed in acoustic resonance measurements.

In 1970, Fleury observed a temperature-dependent

optical mode (at ~ 47 cm^{-1} at 300 K) in the Raman spectrum of GMO in the low-temperature ferroelectric phase (FE), but not in the high-temperature paraelectric phase (PE), and proposed that this mode constituted the essential instability, with the elastic anomaly resulting from a nonlinear interaction between the acoustic phonons and this "soft" optic mode.[30] Subsequent Raman scattering experiments by Ullman and co-workers confirmed Fleury's observation.[31] This soft mode was also observed in far-infrared transmission measurements by Petzelt who found that at temperatures below 0 °C it splits into two distinct components.[32] Kim and Ullman[31] and Shigenari, Takagi, and Wakabayashi[33] later showed that the soft mode observed in the Raman spectrum also exhibits splitting at sufficiently low temperatures. Shigenari *et al.* analyzed their Raman spectra in terms of a two-damped-harmonic-oscillator model, and were able to extract two frequencies for temperatures up to ~ 100 °C.

Later Raman scattering experiments on GMO and TMO by Laiho *et al.*[34] and Sinii *et al.*[35] indicated that the Fleury mode has a low-frequency A_1 partner, that the two modes are separated by ~ 5 cm^{-1} at room temperature, and that both frequencies decrease and both linewidths increase as T is raised towards the transition. Furthermore, they reported a central peak whose intensity increased strongly as the transition was approached.

Recently, Nisar, Garland, and Raccah have also observed two temperature-dependent A_1 modes plus a central peak in the GMO Raman spectrum.[36] Their coupled-mode analysis suggests that the higher-frequency mode persists in the high-temperature (paraelectric) phase, and is therefore not directly involved in the transition. Fleury and Lyons, however, find no evidence of a dynamic central peak outside of the 1-GHz region blocked by their iodine absorption cell, except for the spectral intensity attributable to the Brillouin components.[37]

In 1970 Pytte, drawing on x-ray studies of GMO indicating cell doubling at T_0, proposed that the GMO phase transition is driven by a soft optical mode at the corner of the Brillouin zone, with wave vector in the high-symmetry (PE) phase of $\vec{Q}_M = (\pi/a, \pi/a, 0)$.[38] The same mechanism for the transition was proposed independently by Dvorak[39] and by Levanyuk and Sannikov.[40]

The M-point instability model was confirmed in detail by x-ray and neutron-diffraction experiments. Jeitschko's x-ray structure analysis showed that the FE lattice of GMO is orthohombic with space group C_{2v}^8 and 4 formula units per unit cell, and the PE lattice is tetragonal with space group D_{2d}^3 and 2 formula units.[41] The orthorhombic axes are rotated 45° about z with respect to the tetragonal axes. Dorner, Axe, and Shirane, in an extensive neutron scattering investigation of TMO (the terbium isomorph of GMO) found similar structural results and also observed the temperature-dependent soft mode in PE at the M point and over a large part of the Brillouin zone.[23,24] We note that while the neutron studies of Dorner *et al.* employed TMO, virtually all other experimental studies of the rare-earth molybdates have employed GMO. However, the properties of GMO and TMO should be very similar.

Dorner *et al.* also extended their inelastic neutron scattering studies of the soft mode into the low-temperature FE phase, where the doubly degenerate M-point soft mode is expected to become two nondegenerate zone-center A_1 modes. They found that one mode (called Ω_1) closely resembled the mode reported by Fleury,[30] but with somewhat stronger temperature dependence, and with a room-temperature frequency of 5.7 meV. The eigenvector of this mode was found to be similar to the condensed static displacement η_0. We will henceforth use the term "Fleury mode" in conjunction with the numerical values for $\Omega_1(T)$ found by Dorner *et al.*

The neutron experiments also revealed a central peak at very low frequencies ($\Omega_2 << \Gamma_2 \sim 2$ meV). Dorner *et al.* discussed various possibilities for the identity of the two A_1 modes produced from the doubly degenerate FE soft mode. They concluded that the most natural interpretation of their results is that one of the two modes (Ω_1) is the Fleury mode, and the other (Ω_2) is the central peak.

The neutron, Raman, and infrared results do not conclusively establish the identity of the second soft mode in FE which is the partner of the Fleury mode. We will return to this question in Sec. V where we will use our Brillouin scattering results to test four possibilities.

Following the original investigation by Cross *et al.*[27] and Cummins[28] of the acoustic anomaly in GMO, ultrasonic studies of various GMO elastic constants and absorption coefficients were reported by Epstein, Herrick, and Turek,[42] Chizhikov *et al.*,[43] Agishev *et al.*,[44] Courdille *et al.*[45] (for TMO), and Hochli.[46]

Hochli determined the complete set of temperature-dependent elastic constants in GMO. He also worked out the relations between the two sets of elastic constants appropriate to the two sets of crystallographic axes which are related by a 45° rotation in the xy plane. In his notation, which we shall follow, $\tilde{C}_{ij}$ refers to elastic constants in the paraelectric (PE) axes, and C_{ij} refers to elastic constants in the ferroelectric (FE) axes. The elastic constants C_{11}, C_{22}, $\tilde{C}_{11}$, and $\tilde{C}_{66}$ showed marked anomalies near T_0 with the C_{11} anomaly being most pronounced. These elastic constants decrease gradually as T_0 is approached from above, drop discontinuously at T_0 and then increase again with decreasing T. The other elastic constants (such as C_{33} or C_{66}) are continuous across the transition and exhibit no anomalies within the limits of error of the experiment.

Brillouin scattering studies of GMO have been reported for C_{11} and C_{22} by Itoh and Nakamura,[47,48] and for the full set of elastic constants by Busch, Toledano, and Torres,[49] and by Luspin and Hauret.[50,51] The close agreement between the ultrasonic and Brillouin scattering data shows that there is little dispersion in the sound velocities of GMO, at least up to 10^{10} Hz.

These ultrasonic and Brillouin scattering experiments have been analyzed differently by each author. Busch[49] considered only the effective bilinear coupling in analyzing the FE data, utilizing the full thermodynamic analysis of Dvorak.[39] A similar analysis was given by Esayan *et al.*[44] However, these analyses do not apply to the acoustic anomalies in the PE phase. Luspin and Hauret, on the other hand, concentrated on the PE data.[51] Thermodynamic Green's functions appropriate to the anharmonic $K\epsilon\eta^2$ interaction were calculated and were shown to be consistent with the *form* of the observed anomalies if the soft-mode dispersion curve is assumed to be isotropic. The magnitude of the anomaly was left as an arbitrary scale factor, however, and no attempt was made to include the anomaly in FE in the analysis. Courdille *et al.* analyzed their data for C_{11} and C_{22} (velocity and attenuation) in terms of coupling to the soft mode using parametrized soft-mode dispersion curves.[45] Hochli[46] analyzed his ultrasonic data with both the thermodynamic expressions of Dvorak[39] for the effective bilinear interaction, and with the expressions found by Pytte[20] for the effect of critical fluctuations.

None of these authors attempted to correlate the effects of induced bilinear coupling and critical fluctuations, nor to incorporate the soft-mode dispersion curves of Dorner *et al.* in computing the fluctuation integral. In the next section we will show how these contributions to the elastic anomaly can be combined self-consistently within the framework of Levanyuk's theory,[22] and in Sec. V we will show how this self-consistent analysis can be used to test various models for the soft mode.

III. PHENOMENOLOGICAL THEORY

In this section, we shall outline a phenomenological Landau theory of the ferroelectric phase transition of TMO with particular emphasis on the interaction between the two-dimensional soft mode and the elastic strains. For clarity, we begin by considering the simplest model which would nonetheless retain all the essential physical ideas: an interacting system consisting of one elastic strain ϵ and a one-dimensional soft mode η. In the presence of the interaction, the elastic behavior is modified by two effects which are usually treated separately. The first effect can be derived from the Landau free energy by a straightforward thermodynamic calculation. This results in a morphically induced bilinear coupling which is present only below the phase transition. This part of the procedure is familiar and has been used extensively in ferroelectric phase transitions. The second effect focuses on the influence of soft-mode fluctuations on the elastic behavior. This effect has been treated previously using Green's-function methods by Cowley, Pytte, and others. The complexity of this approach makes it difficult to correlate the two effects in order to describe the full elastic anomaly.

Levanyuk showed that it is possible to incorporate the effect of thermal fluctuations using the Landau theory as a starting point.[22] This approach has the advantage of placing the fluctuation anomaly on the same footing as the bilinear coupling and allows for the unified treatment of the elastic anomaly. In addition, the effect of fluctuations on other thermodynamic quantities can also be easily calculated in this approach.

The model free energy which we shall use initially is:

$$G=\tfrac{1}{2}A\eta^2+\tfrac{1}{4}B\eta^4+\tfrac{1}{6}D\eta^6+\tfrac{1}{2}C_0\epsilon^2-\tfrac{1}{2}K\epsilon\eta^2 \quad . \tag{3.1}$$

The first four terms are the usual expansion in the Landau free energy for η and ϵ in the absence of coupling. The last term describes the third-order nonlinear coupling between the zone-center acoustic mode and pairs of soft optical modes. The constant A which represents the harmonic restoring forces for the optical mode is strongly temperature dependent and extrapolates to zero at a critical temperature T_c: $A=\alpha(T-T_c)$. The other coefficients are assumed to be temperature independent except for the background elastic constant C_0 which is assumed to vary linearly with temperature due to thermal expansion.

The equilibrium values η_0, ϵ_0 for the soft-mode amplitude and the strain are obtained by setting the generalized forces equal to zero:

$$f_\eta=\left(\frac{\partial G}{\partial\eta}\right)_\epsilon=0; \quad \sigma=\left(\frac{\partial G}{\partial\epsilon}\right)_\eta=0 \quad .$$

The resulting equilibrium values η_0 and ϵ_0 are given by

$$\alpha(T-T_c)+\left(B-\frac{K^2}{2C}\right)\eta_0^2+D\eta_0^4=0 \quad , \tag{3.2a}$$

$$\epsilon_0-\frac{K^2}{2C}\eta_0^2=0 \quad , \tag{3.2b}$$

where the second equation has been used in the first to eliminate ϵ_0. Note that for a first-order phase transition (which is appropriate to TMO), it is necessary that $(B-K^2/2C)<0$ and the transition occurs at a temperature $T_0>T_c$ where η and ϵ suffer

discontinuous jumps. The soft mode and strain below the transition are then described by small fluctuations $\delta\eta$, $\delta\epsilon$ about the equilibrium values η_0, ϵ_0. Replacing η by $\eta_0+\delta\eta$ and ϵ by $\epsilon_0+\delta\epsilon$ and making use of Eq. (3.2) to eliminate ϵ_0 in G, we obtain

$$G(\eta_0,\delta\eta,\delta\epsilon)=\frac{1}{2}\left[A+\left[3B-\frac{K^2}{2C_0}\right]\eta_0^2+4D\eta_0^4\right]\delta\eta^2-K\eta_0\delta\epsilon-\frac{1}{2}C_0(\delta\epsilon)^2 \ . \tag{3.3}$$

The elastic constant under zero f_η is then easily shown to be

$$C=\left(\frac{\partial^2 G}{\partial\epsilon^2}\right)_{f_\eta}=\begin{cases}C_0 & (T>T_0)\\ C_0-\dfrac{K^2\eta_0^2}{A+\left[3B-\dfrac{K^2}{2C_0}\right]\eta_0^2+5D\eta_0^4}=C_0-\dfrac{K^2}{2B+4D\eta_0^2} & (T<T_0)\ ,\end{cases} \tag{3.4}$$

where we have used Eq. (3.2) to simplify the equation below the transition. Note that the coupling term has no effect for $T>T_0$ and there is a discontinuous change in C at the phase transition. We now turn to a discussion of thermal fluctuations.

In order to include fluctuation effects, the dynamics of the coupled mode system must be considered. Such an analysis was developed by Sannikov[52] for ferroelectrics of arbitrary crystal symmetry and has been applied to a number of different crystals. We shall show how the thermodynamic result [Eq. (3.4)] is equivalent to the elastic response given by the linearized equations of motion in this dynamical approach in the $\omega\to 0$ limit. The effect of thermal fluctuations is then included by extending the equations of motion beyond the linear approximation and by the judicious use of the fluctuation-dissipation theorem on the resulting equations. In this way, the fluctuation integrals of Pytte will be reproduced.[53]

The dynamical calculation begins with the construction of the Lagrangian density for the system. The potential energy density is taken to be the Landau free energy of Eq. (3.1). The kinetic energy density is

$$T=\frac{1}{2}m^*\dot\eta^2+\frac{1}{2}\rho\dot u^2 \ ,$$

where m^* is the effective mass per unit volume for the soft mode, ρ is the mass density, and u is the local displacement appropriate to the acoustic mode and is related to the elastic strain via $\epsilon=\partial u/\partial r$. Damping is introduced phenomenologically by a Rayleigh dissipation function F:

$$F=\frac{1}{2}m^*\Gamma\dot\eta^2+\frac{1}{2}\rho\gamma\dot u^2 \ ,$$

where Γ and γ represent the damping for the soft mode and the acoustic mode, respectively.

External driving forces are included in the free energy by adding the term

$$G_{\rm ext}=-\epsilon\sigma-\eta f_\eta \ ,$$

where σ and f_η are the stress and driving force associated with the strain and the soft mode. The equations of motion follow from Lagrange's equation for continuous systems:

$$\frac{d}{dt}\left(\frac{\partial L}{\partial\dot\chi}\right)+\frac{d}{dt}\left(\frac{\partial L}{\partial\left(\dfrac{\partial\chi}{\partial r}\right)}\right)-\frac{\partial L}{\partial\chi}+\frac{\partial F}{\partial\dot\chi}=0 \ ,$$

where $\chi=\eta,u$ and $L=T-G-G_{\rm ext}$. The equations of motion are

$$m^*\ddot\eta+A\eta+B\eta^3+D\eta^5-K(\epsilon\eta)+m^*\Gamma\dot\eta=f_\eta \ , \tag{3.5a}$$

$$\rho\ddot\epsilon+\rho\gamma\dot\epsilon-C_0\frac{d^2\epsilon}{dr^2}+\frac{1}{2}K\frac{d^2\eta^2}{dr^2}=-\frac{d^2\sigma}{dr^2} \ . \tag{3.5b}$$

We have differentiated the second equation with respect to r to express u in terms of ϵ.

Note that the equation of motion for η does not include soft-mode dispersion. Dispersion is usually introduced in the Landau theory by the inclusion of a term proportional to $(\nabla\eta)^2$ in the free energy.[54] We have chosen not to do so since it would have fixed the functional form of the soft-mode dispersion. The equation of motion (3.5a) is therefore directly applicable only to the soft mode at the M point. Dispersion will be included later by introducing the empirical results of the neutron scattering experiments of Dorner *et al.*[24]

The frequency response of the coupled mode system is given by the Fourier transform of Eqs. (3.5). The following convention will be followed in Fourier transforming all variables:

$$f(\vec Q,\Omega)=\frac{1}{(2\pi)^4}\int f(\vec r,t)e^{-i(\vec Q\cdot\vec r-\Omega t)}d^3r\,dt \ ,$$

$$f(\vec r,t)=\int f(\vec Q,\Omega)e^{i(\vec Q\cdot\vec r-\Omega t)}d^3Q\,d\Omega \ ,$$

and

$$(2\pi)^4\delta(\vec r)\delta(t)=\int e^{i(\vec Q\cdot\vec r-\Omega t)}d^3Q\,d\Omega \ .$$

The Fourier transforms of Eqs. (3.5) are

$$-m^*\Omega^2\eta(\vec{Q},\Omega)+A\eta(\vec{Q},\Omega)+B\{\eta*\{\eta*\eta\}\}_{\vec{Q},\Omega}+D\{\eta*\{\eta*\{\eta*\{\eta*\eta\}\}\}\}_{\vec{Q},\Omega}$$
$$-K\{\epsilon*\eta\}_{\vec{Q},\Omega}-m^*i\Omega\Gamma\eta(\vec{Q},\Omega)=f_\eta(\vec{Q},\Omega)\ ,$$
$$-\rho\omega^2\epsilon(\vec{q},\omega)-\rho i\omega r\epsilon(\vec{q},\omega)+C_0q^2\epsilon(\vec{q},\omega)-\frac{K^2}{2}q^2\{\eta*\eta\}_{q,\omega}=q^2\sigma(\vec{q},\omega)\ , \tag{3.6}$$

where $\{f*g\}$ denotes the convolution between the functions f and g:

$$\{f*g\}_{\vec{Q},\Omega}=\int d^3Q'd\Omega' f(\vec{Q}',\Omega')g(\vec{Q}-\vec{Q}',\Omega-\Omega')\ .$$

The dynamical variables ($\delta\eta$ for the soft-mode variable and $\delta\epsilon$ for the elastic strain) are small variations of η and ϵ about their equilibrium values η_0' and ϵ_0':

$$\begin{aligned}
&\eta(\vec{Q},\Omega)=\eta_0'(\vec{Q},\Omega)+\delta\eta(\vec{Q},\Omega),\\
&\eta_0'(\vec{Q},\Omega)=\eta_0\delta(\vec{Q}_M-\vec{Q})\delta(\Omega)\ ,\\
&\epsilon(\vec{q},\omega)=\epsilon_0'(\vec{q},\omega)+\delta\epsilon(\vec{q},\omega),\\
&\epsilon_0'(\vec{q},\omega)=\frac{K}{2C_0}\eta_0^2\delta(\vec{q})\delta(\omega)\ .
\end{aligned} \tag{3.7}$$

The equations of motion for the dynamical variables are now derived by substituting Eqs. (3.7) into Eqs. (3.6). In the usual treatment, the equations of motion are linearized by retaining only terms to first order in the dynamical variables.[9] Here we shall also include coupling terms which are second order in the dynamical variables. These added terms will allow us to calculate the elastic anomaly due to thermal fluctuation of the soft mode.

Under harmonic driving forces, the coupled equations of motion for the acoustic branch and the soft optical branch are

$$\frac{1}{\chi_\eta^0}\delta\eta(\vec{Q},\Omega)-K\eta_0\delta\epsilon(\vec{Q}-\vec{Q}_M,\Omega)-K\{\delta\epsilon*\delta\eta\}_{\vec{Q},\Omega}=f_\eta(\vec{Q},\Omega)\ , \tag{3.8a}$$

$$\frac{1}{\chi_\epsilon^0}\delta\epsilon(\vec{q},\omega)-K\eta_0\delta\eta(\vec{q}-\vec{Q}_M,\omega)-\frac{K}{2}\{\delta\eta*\delta\eta\}_{\vec{q},\omega}=\sigma(\vec{q},\omega)\ , \tag{3.8b}$$

where $\chi_\eta^0(\vec{Q},\Omega)$ and $\chi_\epsilon^0(\vec{q},\omega)$ are the zeroth-order susceptibilities for the soft mode and the strain in the absence of coupling:

$$\frac{1}{\chi_\eta^0}(\vec{Q},\Omega)=\left[A+\left(3B-\frac{K^2}{2C_0}\right)\eta_0^2+5D\eta_0^4\right]-m^*\Omega^2-im^*\Omega\Gamma\ , \tag{3.9a}$$

$$\frac{1}{\chi_\epsilon^0}(\vec{q},\omega)=\frac{\rho}{q^2}\left(\frac{C_0q^2}{\rho}-\omega^2-i\omega\gamma\right)\ . \tag{3.9b}$$

In Eqs. (3.8), the various pieces of the argument which was alluded to at the beginning of the section are separated. The first term gives the susceptibilities of the system in the absence of coupling. The second term represents bilinear coupling between the strain and the soft mode. Since it is proportional to η_0, it is nonzero only below the transition. The third term gives the leading nonlinear coupling which will give us the contribution to the elastic anomaly due to fluctuations.

From Eqs. (3.9), the soft-mode frequency Ω_η^2 at the M point is given in terms of the free energy parameters as

$$\Omega_\eta^2(\vec{Q}_M)=\begin{cases}\dfrac{\alpha}{m^*}(T-T_c), & T>T_0\\ \dfrac{1}{m^*}\left[A+\left(3B-\dfrac{K^2}{2C_0}\right)\eta_0^2+5D\eta_0^4\right]=\dfrac{\eta_0^2}{m^*}(2B+4D\eta_0^2), & T<T_0\ .\end{cases} \tag{3.10}$$

We shall incorporate soft-mode dispersion in the subsequent analysis by demanding that the pole of $\chi_\eta^0(\vec{Q},\Omega)$ must correspond to $\Omega_\eta(\vec{Q})$, the observed soft-mode frequency at wave vector $\vec{Q}$ and replace the quantity $[A+(3B-K^2/2C_0)\eta_0^2+5D\eta_0^4]$ in Eq. (3.9a) by $m^*\Omega_\eta^2(Q)$. As discussed above, this procedure should be more accurate than representing dispersion by terms of the form $(\nabla\eta)^2$.

To obtain the elastic susceptibility from Eqs. (3.8), we first multiply Eq. (3.8a) by χ_η^0:

$$\delta\eta(\vec{Q},\Omega)=\chi_\eta^0(\vec{Q},\Omega)[f_\eta(\vec{Q},\Omega)+K\eta_0\delta\epsilon(\vec{Q}-\vec{Q}_M,\Omega)+K\{(\delta\eta)*(\delta\epsilon)\}(\vec{Q},\Omega)]\ . \tag{3.11}$$

Since the final term in Eq. (3.11) is second order in the dynamical variables, we replace $\delta\eta$ in that term by its zeroth-order value [Eq. (3.11) with $\delta\epsilon=0$]:

$$\delta\eta^0(\vec{Q},\Omega)=\chi_\eta^0(\vec{Q},\Omega)f_\eta(\vec{Q},\Omega) \ .$$

The resultant expression for $\delta\eta(\vec{Q},\Omega)$ is then substituted in Eq. (3.8b) yielding

$$\sigma(\vec{q},\omega)=\frac{1}{\chi_\epsilon^0(\vec{q},\omega)}\delta\epsilon(\vec{q},\omega)-K^2\eta_0^2\chi_\eta^0(\vec{q}-\vec{Q}_M,\omega)\delta\epsilon(\vec{q},\omega)-K^2\eta_0\chi_\eta^0(\vec{q}-\vec{Q}_M,\Omega)\{\delta\epsilon*\delta\eta^0\}_{\vec{q}-\vec{Q}_M,\omega}$$
$$-K^2\eta_0\{\delta\eta^0*\chi_\eta^0(\vec{Q}',\Omega')\delta\epsilon(\vec{Q}'-\vec{Q}_M,\Omega')\}_{\vec{q},\omega}-K^2\{\delta\eta^0*\chi_\eta^0(\vec{Q}',\Omega')\{\delta\epsilon*\delta\eta^0\}_{\vec{Q}',\Omega'}\}_{\vec{q},\omega} \ . \quad (3.12)$$

In Eq. (3.12), only terms linear in $\delta\epsilon$ have been retained to yield a linear elastic constant ($\partial\sigma/\partial\epsilon$), and the generalized force $f_\eta(\vec{Q},\Omega)$ has been replaced by $\delta\eta^0(\vec{Q},\Omega)/\chi_\eta^0(\vec{Q},\Omega)$. In order to evaluate the last three terms in Eq. (3.12) which represent nonlinear coupling, we note that according to the fluctuation-dissipation theorem,[49] the time average of $\langle\delta\eta^0(\vec{Q},\Omega)\delta\eta^0(\vec{Q}',\Omega')\rangle$ is given by

$$\langle\delta\eta^0(\vec{Q},\Omega)\delta\eta^0(\vec{Q}',\Omega')\rangle=\frac{kT}{(2\pi)^4\Omega}\chi_\eta^{0\prime\prime}(\vec{Q},\Omega)\delta(\vec{Q}+\vec{Q}')\delta(\Omega+\Omega') \ , \quad (3.13)$$

where $\chi_\eta^{0\prime\prime}$ is the imaginary part of χ_η^0 and $\langle\delta\eta^0(\vec{Q},\Omega)\rangle=0$. Equation (3.12), averaged over the fluctuations in the order parameter, is then reduced to

$$\langle\sigma(\vec{q},\omega)\rangle_{\delta\eta}=\frac{1}{\chi_\epsilon^0(\vec{q},\omega)}\delta\epsilon(\vec{q},\omega)-K^2\eta_0^2\chi_\eta^0(\vec{q}-\vec{Q}_M,\omega)\delta\epsilon(\vec{q},\omega)$$
$$-\frac{K^2}{(2\pi)^4}(kT)\delta\epsilon(\vec{q},\omega)\int d^3Q\frac{d\Omega}{\Omega}\chi_\eta^{0\prime\prime}(\vec{Q},\Omega)\chi_\eta^0(\vec{q}-\vec{Q},\omega-\Omega) \ ,$$

where we have used the δ function in eliminating one of the convolution integrals. The elastic susceptibility including both the effect of bilinear coupling and thermal fluctuation is

$$\frac{1}{\chi_\epsilon(\vec{q},\omega)}=\frac{\partial\langle\sigma(\vec{q},\omega)\rangle_{\delta\eta}}{\partial\epsilon}=\frac{1}{\chi_\epsilon^0(\vec{q},\omega)}-K^2\eta_0^2\chi_\eta^0(\vec{q}-\vec{Q}_M,\omega)$$
$$-\frac{K^2}{(2\pi)^4}kT\int d^3Q\int\frac{d\Omega}{\Omega}\chi_\eta^{0\prime\prime}(\vec{Q},\Omega)\chi_\eta^0(\vec{q}-\vec{Q},\omega-\Omega) \ .$$

The first term on the right-hand side is the inverse susceptibility in the absence of soft-mode coupling. The second term is the result of the linear coupling terms in Eqs. (3.8). Since the soft-mode frequency and damping are much higher than the acoustic frequency,

$$\chi_\eta^0(\vec{q}-\vec{Q}_M,\Omega)\cong\chi_\eta^0(\vec{Q}_M,0)=1/m^*\Omega_\eta^2(\vec{Q}_m) \ .$$

This term reduces to the thermodynamic result for the elastic anomaly. The last term represents the effect of thermal fluctuations and is effective above and below the phase transition. The functional form of the fluctuation integral is identical to the result of Pytte.[20,53] By substituting explicitly for χ_η^0 from Eq. (3.9a), the integration in Ω space of this term can be easily performed using contour integration. The result is

$$\frac{1}{\chi_\epsilon(\vec{q},\omega)}=\frac{1}{\chi_\epsilon^0(\vec{q},\omega)}-\frac{K^2\eta_0^2}{m^*\Omega_\eta^2(\vec{Q}_M)}-\frac{K^2}{m^{*2}}\frac{kT}{(2\pi)^3}\int d^3Q\frac{(1+i\omega/2\Gamma)}{(1-i\omega/\Gamma)\Omega_\eta^2[4\Omega_\eta^2-2i\omega\Gamma(1-i\omega/\Gamma)]} \ .$$

In the case of TMO, since $\omega\ll\Gamma$, the result may be considerably simplified by dropping terms of order ω/Γ, whence,

$$\frac{1}{\chi_\epsilon(\vec{q},\omega)}=\frac{1}{\chi_\epsilon^0(\vec{q},\omega)}-\frac{K^2\eta_0^2}{m^*\Omega_\eta^2(\vec{Q}_M)}-\frac{K^2kT}{m^{*2}(2\pi)^3}\int d^3Q\frac{1}{\Omega_\eta^2(\vec{Q})[4\Omega_\eta^2(\vec{Q})+2i\omega\Gamma(\vec{Q})]} \ .$$

From this formula, we finally identify the elastic constant and the damping as

$$C = C_0 - \frac{K^2\eta_0^2}{m^*\Omega_\eta^2} - \frac{2K^2}{m^{*2}}\frac{kT}{(2\pi)^3}\int \frac{d^3Q}{4\Omega_\eta^4(\vec{Q}) + \omega^2\Gamma^2(\vec{Q})} , \tag{3.14a}$$

$$\gamma = \gamma_0 + \frac{q^2}{\rho}\left[\frac{K^2\eta_0^2}{m^*}\frac{\Gamma}{\Omega_\eta^4} + \frac{K^2}{m^{*2}}\frac{kT}{(2\pi)^3}\int \frac{\Gamma(\vec{Q})d^3Q}{\Omega_\eta^2(\vec{Q})[4\Omega_\eta^4(\vec{Q}) + \omega^2\Gamma^2(\vec{Q})]}\right] . \tag{3.14b}$$

The last terms in Eqs. (3.14) represent the additional contribution to the elastic anomaly due to critical fluctuations. These equations were first derived by Levanyuk in 1966.[22] Because of the presence of $1/\Omega_\eta^4$ in the denominator, the magnitude of the fluctuation integral increases rapidly close to the transition and causes downward bending of the elastic constant both above and below the transition. These equations also show that the magnitude of the fluctuation anomaly and the morphically induced bilinear anomaly are related to each other through the coupling constant K.

In order to analyze the experimental results for TMO, we will have to abandon the simplified free energy employed so far and consider the complete free energy for crystals of the GMO family, including the two-dimensional order parameter and all strains to which it couples, which was worked out by Dvorak[39] from symmetry considerations. With the two components of the order parameter given by $\eta_1 = \eta\sin\phi$ and $\eta_2 = \eta\cos\phi$, this becomes

$$\begin{aligned} G_{\mathrm{PE}} = &\left(\tfrac{1}{2}A\eta^2 + \frac{\eta^4}{4}(B_1 + B_2\cos4\phi + B_3\sin4\phi) + \frac{\eta^6}{6}(D_1 + D_2\cos4\phi + D_3\sin4\phi)\right) \\ &+ [\tfrac{1}{2}\tilde{C}_{11}^0(\tilde{\epsilon}_1^2 + \tilde{\epsilon}_2^2) + \tfrac{1}{2}\tilde{C}_{33}^0\tilde{\epsilon}_3^2 + \tfrac{1}{2}\tilde{C}_{44}^0(\tilde{\epsilon}_4^2 + \tilde{\epsilon}_5^2) + \tfrac{1}{2}\tilde{C}_{66}^0\tilde{\epsilon}_6^2 + \tilde{C}_{12}^0\tilde{\epsilon}_1\tilde{\epsilon}_2 + \tilde{C}_{13}^0(\tilde{\epsilon}_1\tilde{\epsilon}_3 + \tilde{\epsilon}_2\tilde{\epsilon}_3)] \\ &+ \tfrac{1}{2}K_1\eta^2\tilde{\epsilon}_3 + \tfrac{1}{2}K_2\eta^2(\tilde{\epsilon}_1 + \tilde{\epsilon}_2) + \tfrac{1}{2}\eta^2\tilde{\epsilon}_6(K_3\cos2\phi + K_4\sin2\phi) + (\gamma_1 P_3\eta^2\sin2\phi + \gamma_2 P_3\eta^2\cos2\phi) \\ &+ (a_{36}P_3\tilde{\epsilon}_6 + \tfrac{1}{2}\chi_{33}^{-1}P_3^2) . \end{aligned} \tag{3.15}$$

The first three terms in Eq. (3.15) are the Landau free energy of the soft mode. The two-dimensional order parameter is expressed in polar coordinates and is given by its magnitude η and the azimuthal angle ϕ. The next six terms represent the harmonic strain energies. The $\tilde{}$ indicates that the strain and elastic constants $\tilde{C}_{ij}$ are those appropriate to the tetragonal coordinates in PE. The next three terms represent the third-order coupling terms between the order paramter and the various elastic constants which are compatible with the symmetry change (from D_{2d}^3 in PE to C_{2v}^8 in FE). Note that the coupling terms K_3 and K_4 lack the fourfold symmetry of the tetragonal phase and are the cause of the broken symmetry below the transition. The next two terms are the third-order allowed coupling between polarization and the order parameter. The last terms in Eq. (3.15) express the effect of piezoelectric coupling between the polarization P_3 and the xy shear strain $\tilde{\epsilon}_6$.

The free energy derived from symmetry considerations in Eq. (3.15) may be considerably simplified by the known experimental results on these crystals.

(1) The third-order direct coupling between P_3 and η is known to be very small from the experiment on clamped GMO crystals by Cross *et al.*[27] and may be neglected.

(2) The polarization P_3, which is the result of piezoelectric coupling to $\tilde{\epsilon}_6$, can be absorbed into $\tilde{C}_{66}^0$ using the condition that the electric field in the $\hat{z}$ direction should be zero:

$$E_3 = \left(\frac{\partial G}{\partial P_3}\right)_{\tilde{\epsilon}_i,\,\eta,\,\phi} = 0 ,$$

which implies

$$P_3 = \tfrac{1}{2}a_{36}\tilde{\epsilon}_6\chi_{33} .$$

The polarization P_3 will be dropped from the discussion.

(3) The available data on the elastic constants of GMO show that the elastic anomaly for $\tilde{C}_{33}$ is small in comparison with those of $\tilde{C}_{11}$ and $\tilde{C}_{66}$.[46,50,55] We assume in the following discussion that K_1 is zero.

(4) The elastic strains $\tilde{\epsilon}_3$, $\tilde{\epsilon}_4$, and $\tilde{\epsilon}_5$ are not coupled to the soft mode and will be dropped as they are not relevant to the discussion of the elastic

anomalies.

(5) The soft modes are degenerate in PE and the two linearly independent branches are defined to within a rotation about the $\hat{z}$ axis. We shall pick the axes so that the coupling term between η and $\tilde{\epsilon}_6$ has the form $K_3\eta^2\epsilon_6\cos2\phi$.

With these approximations, Eq. (3.15) is reduced to

$$G_{\rm PE}=\tfrac{1}{2}A\eta^2+\frac{\eta^4}{4}(B_1+B_2\cos4\phi+B_3\sin4\phi)+\frac{\eta^6}{6}(D_1+D_2\cos4\phi+D_3\sin4\phi)$$
$$+[\tfrac{1}{2}\tilde{C}^0_{11}(\tilde{\epsilon}_1^2+\tilde{\epsilon}_2^2)+\tfrac{1}{2}\tilde{C}^0_{66}\epsilon_6^2+\tilde{C}^0_{12}\tilde{\epsilon}_1\tilde{\epsilon}_2]+\tfrac{1}{2}K_2\eta^2(\tilde{\epsilon}_1+\tilde{\epsilon}_2)+\tfrac{1}{2}K_3\cos2\phi\eta^2\tilde{\epsilon}_6\ . \tag{3.16}$$

This form of the free energy is similar to that used by Hochli[41] in his thermodynamic discussion. The nature of the spontaneous displacement has been considered by several authors[24,39] using thermodynamics on $G_{\rm PE}$. They concluded that all experimental data are consistent with the assumption that the direction of the spontaneous displacement is temperature independent.

The dynamical analysis can now be performed following the outline used for the one-dimensional case. We shall be primarily interested in the elastic behavior of $\tilde{\epsilon}_1$. There are two added features in using the full free energy: (1) the presence of the other elastic constants, and (2) the two dimensionality of the soft mode. For the first point, the analysis of the Lagrangian density shows that the equations of motion for $\tilde{\epsilon}_1$ and $\tilde{\epsilon}_2$ are identical and are decoupled from $\tilde{\epsilon}_6$. The equation of motion for $\tilde{\epsilon}_1$ is essentially the same as for a one-dimensional system. As for the second point, since the soft mode is in general nondegenerate below the phase transition, it is necessary to choose the dynamical variables $\delta\vec{\eta}_1$ and $\delta\vec{\eta}_2$ as those appropriate to the two nondegenerate branches. An expansion of the coupling term $K_2\vec{\eta}^{\,2}\tilde{\epsilon}_1$ with $\vec{\eta}=\vec{\eta}_0+\delta\vec{\eta}_1+\delta\vec{\eta}_2$ yields

$$K_2\vec{\eta}^{\,2}\tilde{\epsilon}_1=K_2\eta_0^2\tilde{\epsilon}_1+2K_2(\vec{\eta}_0\cdot\delta\vec{\eta}_1)\tilde{\epsilon}_1$$
$$+2K_2(\vec{\eta}_0\cdot\delta\vec{\eta}_2)\tilde{\epsilon}_1+K_2\delta\eta_1^2\tilde{\epsilon}_1+K_2\delta\eta_2^2\tilde{\epsilon}_1\ .$$

The presence of $(\vec{\eta}_0\cdot\delta\vec{\eta}_1)$ and $(\vec{\eta}_0\cdot\delta\vec{\eta}_2)$ follows from the fact that in two dimensions it is generally not necessary that the spontaneous displacement $\vec{\eta}_0$ and either of the dynamical variables $\delta\vec{\eta}_1$ and $\delta\vec{\eta}_2$ be in the same direction. Only that part of each dynamical variable which is in the direction of the spontaneous displacement will lead to a morphically induced bilinear coupling. This has the effect of reducing the magnitude of the bilinear anomaly for each soft-mode branch relative to the magnitude of the corresponding fluctuation anomaly. Since the values of $(\vec{\eta}_0\cdot\delta\vec{\eta}_1)$ and $(\vec{\eta}_0\cdot\delta\vec{\eta}_2)$ are not known from any other experiment, we shall initially make the usual assumption[24] that $\vec{\eta}_0\perp\delta\vec{\eta}_2$ and $\vec{\eta}_0\parallel\delta\vec{\eta}_1$. In this case, the elastic anomaly is

$$\tilde{C}_{11}=\tilde{C}^0_{11}-\frac{K_2^2\eta_0^2}{m^*\Omega^2_{\eta_1}}-\frac{2K_2^2kT}{(2\pi)^3m^{*2}}\left[\int\frac{d^3Q}{4\Omega^4_{\eta_1}(\vec{Q})+\omega^2\Gamma_1^2(\vec{Q})}+\int\frac{d^3Q}{4\Omega^4_{\eta_2}(\vec{Q})+\omega^2\Gamma_2^2(\vec{Q})}\right]\ , \tag{3.17}$$

where $\Omega_{\eta_1}(\vec{Q})$ is the frequency for vibration along the spontaneous displacement and $\Omega_{\eta_2}(\vec{Q})$ is the frequency for vibration perpendicular to the spontaneous displacement (i.e., modes with eigenvectors parallel to and perpendicular to $\vec{\eta}_0$).

The elastic constants C_{11} and C_{22} of the molybdates also show appreciable anomalies. It is of interest to work out the elastic anomalies for these cases also. In this case, it is necessary to reexpress the free energy in terms of elastic constants and elastic strains appropriate to FE. The transformation between the elastic constants of PE and FE have been carried out by Höchli.[41] The result is

$$G_{\rm FE}=\tfrac{1}{2}A\eta^2+\frac{\eta^4}{4}(B_1+B_2\cos4\phi+B_3\sin4\phi)+\frac{\eta^6}{6}(D_1+D_2\cos4\phi+D_3\sin4\phi)$$
$$+\tfrac{1}{2}C^0_{11}(\epsilon_1^2+\epsilon_2^2)+C^0_{12}\epsilon_1\epsilon_2+(K_2+K_3\cos2\phi)\eta^2\epsilon_1+(K_2-K_3\cos2\phi)\eta^2\epsilon_2\ . \tag{3.18}$$

Note that in carrying out the transformation from PE coordinates to FE coordinates, ϵ_6 is uncoupled from the soft mode and has been dropped from the free energy as irrelevant.

In deriving the anomalies of C_{11} and C_{22}, we continue to assume that $\delta\vec{\eta}_1 \| \vec{\eta}_0$ and $\delta\vec{\eta}_2 \perp \vec{\eta}_0$. The dynamical analysis for C_{11} and C_{22} closely parallels the analysis for $\tilde{C}_{11}$ though the angular dependence in $K_3\cos 2\phi$ makes the calculation somewhat more elaborate. Here we briefly discuss the coupling terms for C_{11} to motivate the results for the elastic anomaly for C_{11} and C_{22}. The coupling terms for ϵ_1, expanded about the equilibrium position η_0, ϕ_0 are

$$G_{\mathrm{FE}} = \cdots + [2(K_2 + K_3\cos 2\phi_0)\eta_0\delta\eta_1\epsilon_1 - 2K_3\sin 2\phi_0\eta_0\delta\eta_2\epsilon_1]$$
$$+ [(K_2 + K_3\cos 2\phi_0)\delta\eta_1^2\epsilon_1 + (K_2 - 2K_3\cos 2\phi_0)\delta\eta_2^2\epsilon_1 - 3K_3\sin 2\phi_0\delta\eta_1\delta\eta_2\epsilon_1] + \cdots .$$

The terms in the first set of brackets above are the morphically induced bilinear coupling and the terms in the second brackets are the third-order coupling terms associated with fluctuations. Note that there is an induced bilinear coupling to $\delta\eta_2$ even though $\vec{\delta}\eta_2 \perp \vec{\eta}_0$. This is because the effective coupling constant $K_3\cos 2\phi$ is angle dependent. The last term in the third order nonlinear coupling is a cross term between $\delta\eta_1$ and $\delta\eta_2$. As the fluctuations in $\delta\eta_1$ and $\delta\eta_2$ are not correlated, this term gives no contribution. With this observation, we may write the elastic anomaly for C_{11} and C_{22}:

$$C_{11} = C_{11}^0 - \frac{(K_2 + K_3\cos 2\phi_0)^2\eta_0^2}{m^*\Omega_{\eta_1}^2(\vec{Q}_M)} - \frac{(K_3\sin 2\phi_0)^2\eta_0^2}{m^*\Omega_{\eta_2}^2(\vec{Q}_M)} - 2\frac{(K_2 + K_3\cos 2\phi_0)^2}{(2\pi)^3 m^{*2}}(kT)\int \frac{d^3Q}{4\Omega_{\eta_1}^4(\vec{Q}) + \omega^2\Gamma^2}$$
$$- 2\frac{(K_2 - K_3\sin 2\phi_0)^2}{(2\pi)^3 m^{*2}}(kT)\int \frac{d^3Q}{4\Omega_{\eta_2}^4(\vec{Q}) + \omega^2\Gamma^2} ,$$
$$C_{22} = C_{22}^0 - \frac{(K_2 - K_3\cos 2\phi_0)^2\eta_0^2}{m^*\Omega_{\eta_1}^2(\vec{Q}_M)} - \frac{(K_3\sin 2\phi_0)^2\eta_0^2}{m^*\Omega_{\eta_2}^2(\vec{Q}_M)} - 2\frac{(K_2 - K_3\cos 2\phi_0)^2}{(2\pi)^3 m^{*2}}(kT)\int \frac{d^3Q}{4\Omega_{\eta_1}^4(\vec{Q}) + \omega^2\Gamma^2} \tag{3.19}$$
$$- 2\frac{(K_2 + K_3\cos 2\phi_0)^2}{(2\pi)^3 m^{*2}}(kT)\int \frac{d^3Q}{4\Omega_{\eta_2}^4(\vec{Q}) + \omega^2\Gamma^2} .$$

The formula for C_{22} differs from that for C_{11} only in the replacement of K_3 by $-K_3$ as is clear from Eq. (3.18).

IV. EXPERIMENT

Single crystals of TMO were provided by Barkley and Brixner of the Central Research Department of E. I. DuPont de Nemours and Company, Inc. From these, two separate samples of TMO were cut and polished for the Brillouin measurements of $\tilde{C}_{11}$ and C_{11}, C_{22}. The size of both samples was approximately $6 \times 4 \times 6$ mm^3. The sample for $\tilde{C}_{11}$ measurements has faces perpendicular to the FE axes and the sample for the C_{11}, C_{22} measurements has faces perpendicular to the PE axes. Single-domain samples were obtained by poling at the start of the experiment. Data were taken during both the heating and the cooling phases of the experiments and no hysteresis effects were noticed. After the experiment, the samples were found to be multidomain when examined under crossed polaroids.

Since no changes in the Brillouin shifts were seen between the heating and cooling cycle, the effects of residual strains due to domains on the elastic constants are apparently small. Therefore, we did not attempt to pole the crystals during the experiments.

The sample was located in a small copper oven for temperature control. The oven consists of three concentric layers. The sample itself is surrounded by a small copper block machined to fit the sample closely to minimize heat loss due to thermal convection. A hole was drilled in this block to receive a platinum resistance thermometer which is used to measure the temperature of the crystal.[56] This copper block is surrounded completely by a glass enclosure which serves to isolate the sample and the inner block from the temperature gradients around the external heater elements. The glass enclosure is itself embedded in another copper block into which holes have been drilled for six $\frac{1}{8}$-in.-diam $\times$ 1-in. cartridge heaters[57] and a small thermistor.[58] These are connected to a Fisher Model 22 proportional temperature controller as heating and sensing elements. Holes were drilled

in both the inner and outer copper block to provide optical access to the sample. The complete oven assembly is suspended in the center of a stainless-steel cross with window flanges which is evacuated and backfilled with oxygen for the experiment. This is necessary as oxygen diffuses freely out of molybdate crystals upon heating unless they are kept under an oxygen atmosphere.[59] The entire chamber may be translated along all three axes to select the region in the crystal where parasitic elastic scattering is a minimum.

The Brillouin scattering apparatus used in this experiment is shown in block diagram form in Fig. 1. Light from a Coherent Radiation Model 52 argon ion laser (30 mW nominal single-mode power at 5145 Å) was focused onto the sample and the scattered light was collected at 90°. The incoming laser light was polarized perpendicular to the scattering plane; the polarization of the scattered light was not analyzed. The scattered light was collimated and passed through a spatial filter which serves to define the scattering volume. The size of the pinhole in the spatial filter was chosen to match the image of the scattering column in the focal plane. The scattered light from the region of the crystal defined by the spatial filter was then analyzed with a Tropel Model 350 piezoelectrically scanned triple pass Fabry-Perot interferometer. The Fabry-Perot plates were matched and rotated to achieve maximum parallelism in those regions of the plates which are utilized in triple-pass operation. The Fabry-Perot has a typical finesse of 50 and a contrast of 4×10^6. Several spacings corresponding to free spectral ranges from 26.5 to 31.2 GHz were used to cover the entire range of sample temperatures. The output of the Fabry-Perot was focused on another pinhole before being imaged onto an ITT FW130 phototube. A narrow-band laser filter was placed in front of the phototube to eliminate the Raman scattering intensity.

Photon counting was used in the detection system and the data were stored in a PDP 8/e minicomputer used as a multichannel analyzer. A total of 512 24-bit memory channels were used in this experiment. The counting time per channel was set so that the 512 channels cover approximately two free spectral ranges. Figure 2 shows a typical spectrum obtained. Sequential scans were taken to build up the Brillouin components until a satisfactory signal-to-noise ratio was obtained. The peak-to-peak ramp voltage (set typically at 400 V) was chosen to cover approximately 2.5 free spectral ranges during the five-second ramp duration. It is necessary to set the ramp voltage to scan over more orders than are actually used in the data acquisition to allow for drifts in the laser frequency or the interferometer during the accumulation of data.

The high contrast of the triple-pass Fabry-Perot is needed because of the poor optical quality of the crystals. In our TMO samples, the Brillouin components were typically 10^5 times weaker than the Rayleigh lines. During the data runs, the phototube must be protected from exposure to the intense Rayleigh line, so a fast electonic shutter assembly is included in the optics.[60] During a typical data sweep, the number of incoming counts to each channel is monitored by the computer. When the count rate increases beyond a preset limit the shutter is closed for a sufficient number of channels (which can also

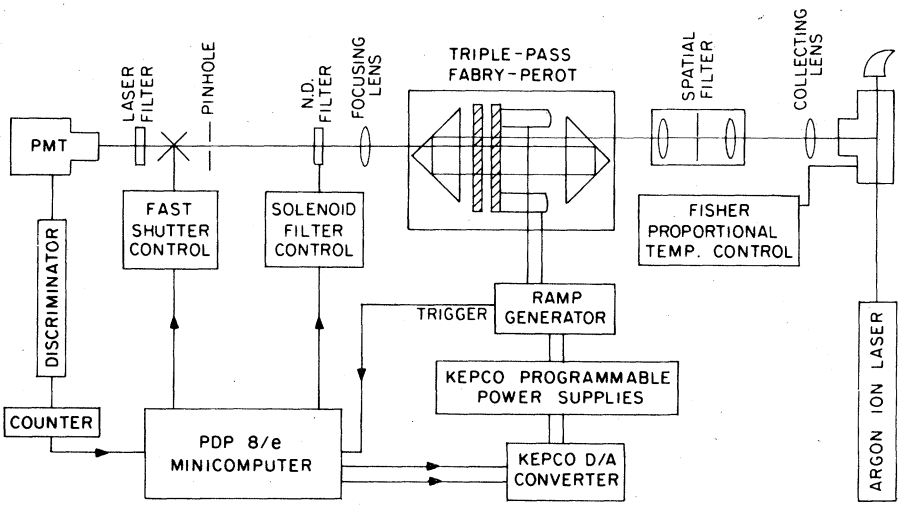

FIG. 1. Schematic diagram of the Brillouin scattering apparatus. The programmable power supplies are connected in series with the output of the ramp generator and provide additional bias under computer control. Timing for the data scan is provided by the ramp generator trigger signal at the start of each ramp cycle. Details of the operating program are discussed in the text.

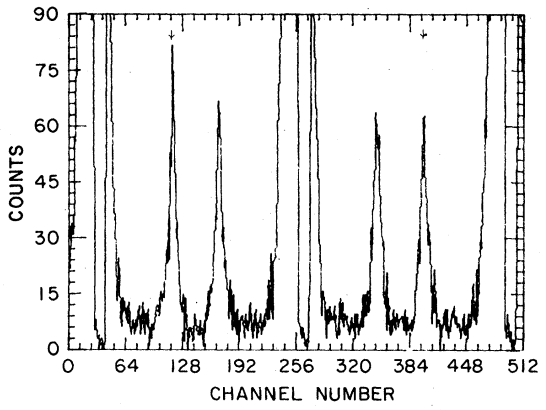

FIG. 2. Representative Brillouin spectrum of TMO approximately 1 K above the phase transition. The two outer Brillouin lines (↓) are the Stokes and anti-Stokes components associated with the central Rayleigh peak. The low count rate region at the center of the Rayleigh line shows the fast shutter in action during data scans. Full scale: 90 counts. Free spectral range: 1.56 cm^{-1}.

be specified) to block out the Rayleigh peak.

The minicomputer is also used to maintain the alignment of the Fabry-Perot in the course of a long data run. It was found that the quality of the collected data degraded noticeably after 5 min of continuous operation. The computer periodically interrupts the data acquisition and realigns the Fabry-Perot. During the alignment routine the computer first actuates a relay which inserts a solenoid-operated neutral-density filter in the optical path. This reduces the peak intensity of the Rayleigh line to below the threshold set for the shutter to close. The computer then examines the count rate at the Rayleigh peak and adjusts the bias voltages for maximum signal. The adjustment of the bias is done through two Kepco OPS-500 programmable power supplies which are connected in series with the bias controls of two of the three piezoelectric stacks. These are located at 90° with respect to the third stack which serves as the pivot of the motion, which ensures that the two adjustments are independent. The computer controls the output of the programmable power supplies through two Kepco SN-8 D to A converters. At the start of the alignment routine, the computer first locates and stores the size and location of the Rayleigh line near the center of the sweep. At each subsequent sweep, the computer changes the bias voltage by a fixed increment. If the size of the Rayleigh peak has increased from the previous cycle, the new bias voltage is retained and the same process repeated on the next cycle. If the size of the Rayleigh peak was reduced, the new bias voltage is rejected and the program continues to the next alignment phase. During the alignment routine, the above process is repeated for both stacks and for voltage increments

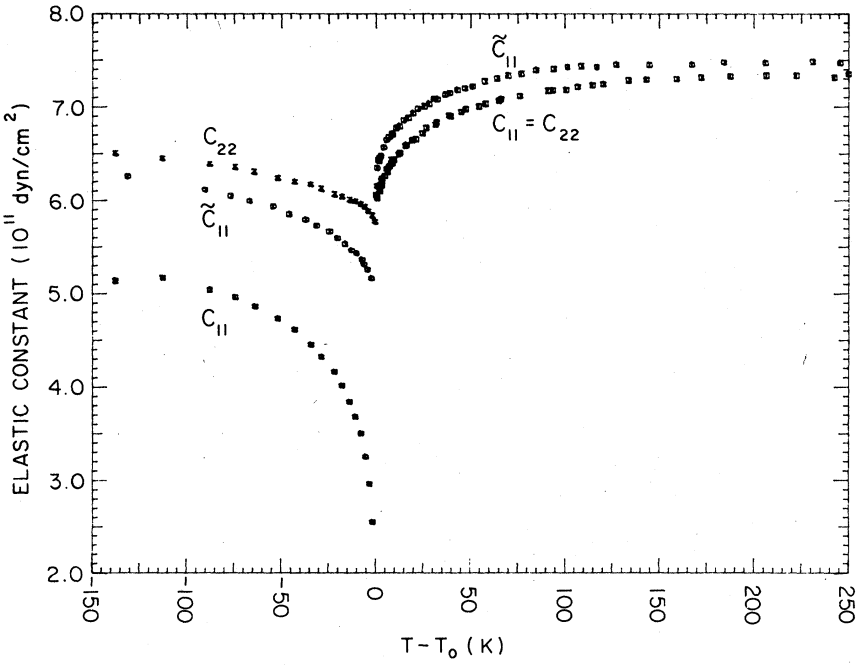

FIG. 3. Elastic constants of TMO derived from Brillouin scattering data. $\tilde{C}_{11}$ is the elastic constant for longitudinal waves traveling in the x direction of the paraelectric crystalline axes. C_{11} and C_{22} are the elastic constants for longitudinal waves traveling in the x and y directions of the ferroelectric crystalline axes.

of both polarities. At the end of the cycle, the position of the Rayleigh peak with respect to the center of the sweep is recorded and used to update a variable delay which ensures that the collected spectrum is always centered in the 512 channels. Acquisition time for a typical spectrum in this experiment was about 30 min. This corresponds to a total time per bin of approximately 1.5 sec. Data runs as long as 4 h were used during testing, and no degradation in the instrumental finesse was observed.

XY plots were made of the digital data in the computer and the results were analyzed by hand to obtain the Brillouin shift. Close to the transition, significant broadening of the Brillouin components was observed. Whenever the broadening produced noticeable asymmetry in the line shape, the data were rejected. Otherwise, the Brillouin shift was taken to be given by the peak position. The Brillouin shifts deduced in this way were found to be reproducible to within 0.3%. Figure 3 shows the elastic constants $\tilde{C}_{11}$, C_{11}, and C_{22} of TMO derived from the Brillouin experiment.

V. DATA ANALYSIS AND DISCUSSION

In Sec. III, Eqs. (3.17) and (3.19) which govern the elastic anomalies of $\tilde{C}_{11}$, C_{11}, and C_{22} in TMO were derived. There are two consequences of the anharmonic coupling to the soft mode: (1) a bilinear coupling in the FE phase induced by the condensation of the soft mode, and (2) a quadratic coupling of the soft mode to the thermal fluctuations which occurs in both PE and FE phases. The absence of the bilinear coupling simplifies the analysis of the acoustic anomaly above the transition. Using the known soft-mode characteristic, we first analyze the data in PE according to Eq. (3.17) and obtain numerical value for the coupling constant K_2. The value of K_2 will allow us to calculate the expected magnitude for the total anomaly below the transition and compare it with our experimental result.

In carrying out this program, we shall rely heavily on the soft-mode characteristics determined in the neutron experiments of Dorner *et al.*[23,24] Though the neutron data are quite extensive, a number of parameters relevant to the analysis are not available and have been left as free parameters. Above the phase transition, the frequency dependence of the doubly degenerate soft mode at the M point was found to be described over a wide temperature range by

$$\Omega_\eta^2 = 0.0165(\text{meV}^2/^\circ\text{C})(T - 149\,^\circ\text{C}) \ .$$

Below the transition, the doubly degenerate soft mode may be split into two distinct branches.

The zone-center frequency of one of the two branches will be assumed to be the 5.7-meV "Fleury mode" with temperature dependence shown in Fig. 8 of Dorner *et al.*[24] As discussed in Sec. II, this mode has been observed in neutron, Raman, and infrared absorption experiments, although with somewhat different frequencies. Several possibilities for the second branch will be considered below.

The damping of the soft mode in PE and FE was also determined in the neutron experiment. Using these values, we find that damping would have negligible effect on the value of the fluctuation integral in Eq. (3.17). In the present formalism soft-mode damping leads to acoustic dispersion in the elastic anomaly through the term $\omega^2\Gamma^2$ in the denominator of the fluctuation integral. Since no significant differences were found between the Brillouin and ultrasonic experiments, we shall drop $\omega^2\Gamma^2$ from the fluctuation integral in the following analysis.

In analyzing the data below the phase transition, the amplitude η_0 of the condensed soft mode will also be needed. As this information is not available for TMO, we shall rely on experiments done on GMO which is structually isomorphic to TMO. The shear angle,[28] the spontaneous polarization,[28] and the Bragg intensity of the superstructure peaks[41] are all measures of the amount of distortion from PE and are proportional to η_0^2. The value of η_0^2 relative to its value at the transition may be determined from the relative temperature dependence of these quantities. Dorner *et al.* have shown that good agreement is obtained with the prediction of the Landau free energy in all three cases, and the ratio of $\eta_0^2(T)$ to $\eta_0^2(T_0)$ is

$$\frac{\eta_0^2(T)}{\eta_0^2(T_0)} = \frac{1}{3}\left[2 + \left[4 - 3\frac{T - T_c'}{T_0 - T_c'}\right]^{1/2}\right] = R(T) \ , \quad (5.1)$$

where T_0 is the transition temperature. Good fits were obtained to all experiments with $T_0 - T_c' = (3 \pm 1)$ K. The critical temperature determined in this way differs from that obtained by extrapolating the soft-mode frequency to zero which gives $T_0 - T_c = (11 \pm 2)$ K. The absolute magnitude of η_0 is determined from the measurement by Jeitschko[41] of the displacement of the atoms under switching at room temperature. Using the individual atomic displacements, we found that η_0 at room temperature is 1.65 Å. The same x-ray study also shows that only oxygen atoms are involved in the distortion from tetragonal to orthorhombic symmetry. The effective mass of the associated soft mode is particularly simple and is equivalent to treating the soft mode as involving only the vibration of a single oxygen atom per unit cell. Using the values of the lattice constants for TMO given in the neutron work, we found $m^* = 0.0461$ g/cm^3.

To carry out the integration of the fluctuation integral, the dispersion curve of the soft-mode branch is needed. The results of Dorner *et al.* indicate that the dispersion curve is nearly isotropic in the xy plane in Q space. The dispersion in this plane is fixed by

measurement of the soft mode along the xy diagonal. Along this direction, the temperature dependence of Ω_η diminishes as one move away from the M point and it becomes temperature independent beyond the half-way point to the origin. Unfortunately, the dispersion curves are not complete since no data are available along the z direction.

Following Miller and Axe[7] and Luspin and Hauret[51] we assume a dispersion relation of the form:

$$\Omega_\eta^2(\vec{Q}_M + Q_r\hat{r} + Q_z\hat{z}) = \Omega_\eta^2(\vec{Q}_M) + \zeta_r Q_r^2 + \zeta_z Q_z^2 \ ,$$

where $\hat{r}$ is a unit vector in the xy plane in Q space. ζ_r at all temperatures is fixed by adjusting it so that $\Omega_\eta(Q_M + Q_r\hat{r}) = 4$ meV if $Q_r \geq \frac{1}{2}|Q_M|$ (see Fig. 3 of Ref. 24). We assume that the z dispersion ζ_z is similarly determined by

$$\Omega_\eta(\vec{Q}_M + Q_z\hat{z}) = \text{const} = C_z \text{ for } Q_z \geq \tfrac{1}{2}|Q_M|$$

at all temperatures. Since in this case no data are available, C_z will be treated as a free parameter. As for the integration volume, it is convenient to choose a Brillouin zone centered about $\vec{Q}_M$. Because of the factor of $\Omega_\eta^4(Q)$ in the denominator, the integral is weighted heavily towards points close to the M point, and one expects that the shape of the zone boundary would not be crucially important. For simplicity, the integration volume is chosen as a circular cylinder with a radius of $t|Q_M|$ and a height of $2t|Q_M|$ where t has been chosen to match the volume of the correct Brillouin zone. A spherical integration volume was also tried with only minor modification to the result.

Besides the soft-mode characteristics listed above, we shall also need to infer from the experiment what the background elastic constant should be in the absence of coupling to the soft mode. We assume that the background elastic constant $\tilde{C}_{11}^0(T)$ is a linear function of temperature and characterize it by its value at the transition $\tilde{C}_{11}^0(T_0)$ and its temperature slope $(\partial\tilde{C}_{11}^0/\partial T)$. We treat both the background and its slope as free parameters. This is at variance with the procedure used by Luspin and Hauret[46] who obtained the elastic constants of GMO up to 800 °C and found that the elastic constant decreases linearly above 600 °C. They argued that the background elastic constant should be extrapolated from the high-temperature experimental data. However, conversations with Dr. John Barkley of Du Pont have cast doubt upon this procedure. The β phase of the molybdate family which is responsible for the ferroelectricity is only metastable at room temperature. As the crystal is heated beyond 700 °C, significant nucleation of the crystal into the more stable α phase is observed and it is not clear how the competition between the two phases will affect the elastic behavior at high temperature. The background elastic constant determined in our fitting procedure shows considerably less temperature dependence than that used by Luspin and Hauret.

For clarity in presentation, we have grouped above all the parameters relevant to the data analysis both above and below T_0. For $T > T_0$, only those characteristics which pertain to the PE phase are required. These include the soft-mode frequency, its dispersion, and the effective mass of the soft mode. The elastic constant $\tilde{C}_{11}$ in terms of the soft-mode parameters is given by Eq. (3.17) (after dropping the damping terms) as

$$\tilde{C}_{11} = \tilde{C}_{11}^0 - \frac{K_2^2 kT}{(2\pi)^3 m^{*2}} \int \frac{d^3Q}{\Omega_\eta^4(T)} \ . \tag{5.2}$$

This leaves us with four independent parameters: $\tilde{C}_{11}^0(T_0)$, $(\partial\tilde{C}_{11}^0/\partial T)$, K_2^2, and C_z. We show in Fig. 4 the best fit to the experimental data when all four parameters are allowed to vary freely.

An error analysis of the fit of Eq. (5.2) to the experimental data in PE shows that K_2 and C_z are strongly correlated. Because of this, we have carried out an analysis with C_z fixed at different values and allowed the other three parameters to vary in obtaining the minimum χ^2 deviation. The error limits on the parameters given below signify the values at which the χ^2 deviation of the overall fit is doubled from its minimum in this fitting procedure. The big-

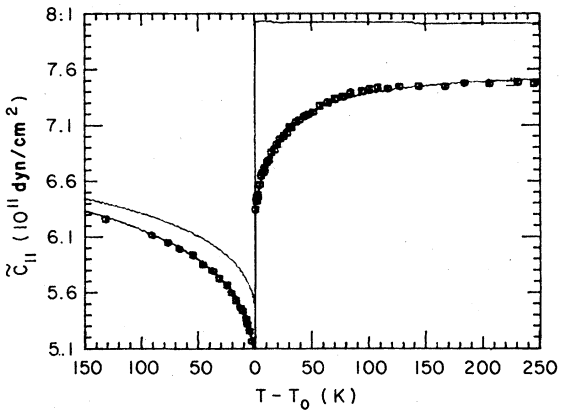

FIG. 4. Results of the fit of the elastic constant $\tilde{C}_{11}$ of TMO to model 3. In the temperature range above T_0, the upper curve shows the background elastic constant $\tilde{C}_{11}^0$ which would apply in the absence of coupling to the soft mode; the lower curve is the result of fitting the elastic constant data for $T > T_0$ to Eq. (5.2). The data below T_0 were fitted to Eq. (3.17) assuming that the eigenvector of the "missing" soft mode is parallel to the spontaneous displacement and the eigenvector of the "Fleury" mode is perpendicular to it (model 3). The upper curve represents the effect of the induced bilinear coupling alone while the lower curve includes the effects of both the bilinear coupling and the anharmonic coupling to critical fluctuations. The results of this fit for $T > T_0$ coincide with the curve shown to within experimental error.

gest uncertainties in the parameters are in K_2^2 and C_z. The value of the background elastic constant was not strongly affected by the uncertainty in C_z:

$$\tilde{C}_{11}^0(T) = [(8.07 \pm 0.07) - (0.000\,23 \pm 0.000\,30) \times (T - T_0)] \times 10^{11}\ \text{dyn/cm}^2 \ .$$

$\tilde{C}_{11}^0(T)$ derived from our fitting is essentially temperature dependent within experimental error and the upper limit on the slope is an order of magnitude smaller than that used in the analysis by Luspin and Hauret.

The limits on the value of C_z were found to be $1 < C_z < 24$ meV. These limits are consistent with isotropic dispersion ($C_z = 4$ meV) for the soft mode. The data are qualitatively different from and inconsistent with a two-dimensional dispersion ($C_z = 0$) as discussed by Pytte[20] and by Luspin and Hauret.[51] Although no relevant neutron data exist, it has been suggested that the soft-mode dispersion should be nearly isotropic on physical grounds.[61]

The best fit to the experimental data is obtained with $K_2^2 = 0.24 \times 10^{52}(\text{dyn/cm}^4)^2$. The corresponding limits on its value are

$$0.10 < K_2^2 < 0.40 [\times 10^{52}(\text{dyn/cm}^4)^2] \ .$$

Note that over the same temperature range, the uncorrelated variable $K_2^2/\sqrt{C_z}$ varies over much smaller limits:

$$0.08 < K_2^2/\sqrt{C_z} < 0.10\,[\times 10^{52}(\text{dyn/cm}^4)^2/(\text{meV})^{1/2}] \ .$$

Having obtained the value of the coupling constant K_2 above the phase transition, we are now in a position to examine the data below the phase transition. We shall assume that the Landau free energy which was derived in the paraelectric phase continues to be valid when expanded about the equilibrium position in the low-temperature phase. We also assume that the background elastic constant $\tilde{C}_{11}^0(T)$, which represents the elastic behavior in the absence of coupling, may be extended smoothly into the ferroelectric phase. The elastic anomaly is then given by the difference between the experimental $\tilde{C}_{11}(T)$ and the extrapolated background.

Below T_0, the twofold degeneracy of the soft mode may be lifted by the symmetry breaking, and the elastic anomalies due to the two soft-mode branches must be treated separately. We are now forced to make some assumptions about the nature of these two branches in order to carry out the analysis. Four distinct models will be considered which appear to cover all proposed interpretations.

Model 1: The two zone-center modes are nearly degenerate in the low-symmetry phase. *Model 2:* The Fleury mode is the longitudinal mode (eigenvector parallel to $\vec{\eta}_0$). The transverse mode is a very-low-frequency excitation which lies within the central peak. *Model 3:* The Fleury mode is the transverse mode while the longitudinal mode has arbitrary temperature dependence. *Model 4:* The two modes are degenerate at room temperature with the frequency of one given by the Fleury mode. The two orthogonal eigenvectors are oriented at an arbitrary angle ψ relative to $\vec{\eta}_0$.

Model 1, which corresponds to the interpretation of Sinii *et al.*,[34,35] is the most straightforward to analyze. The elastic anomaly in the low-symmetry phase ($T < T_0$) is first expressed as the sum of two terms:

$$\Delta\tilde{C}_{11} = \tilde{C}_{11}^0 - \tilde{C}_{11} = \Delta\tilde{C}_{11}^L + \Delta\tilde{C}_{11}^F \ ,$$

where $\Delta\tilde{C}_{11}^L$ and $\Delta\tilde{C}_{11}^F$ denote the bilinear and fluctuation anomalies, respectively,

$$\Delta\tilde{C}_{11}^L = \frac{K_2^2\eta_0^2}{m^*\Omega_\eta^2}; \quad \Delta\tilde{C}_{11}^F = \frac{K_2^2 kT}{(2\pi)^3 m^{*2}} \int \frac{d^3Q}{\Omega_\eta^4(\vec{Q})} \ . \tag{5.3}$$

As in the PE phase, the two dimensionality of the soft-mode results in a doubling of the fluctuation anomaly. However, the induced bilinear coupling is not doubled since it is only effective for that part of the soft mode which is in the direction of the spontaneous displacement. In Fig. 5 we show the experimental values of Ω_η in PE and FE taken from the neutron scattering results. Above the phase transition, the soft mode varies in frequency from 0.4 meV at the transition to 1.3 meV at about 100 °C above T_0. Below T_0, Ω_η is much higher and varies from 5.7 meV at room temperature to 2.7 meV at T_0. The effect of critical fluctuations ($\Delta\tilde{C}_{11}^F$) at these higher frequencies is much reduced from its value in the high-temperature phase and varies from 0.06×10^{11} dyn/cm^2 at room temperature to 0.15×10^{11} dyn/cm^2 at T_0. In evaluating the fluctuation integral, the integration is now over a Brillouin zone which is half the size of that in PE because of the doubling of the unit cell. At the same time, each soft-mode branch would become two branches in the smaller zone. An equivalent treatment which we shall adopt is to continue to use the PE Brillouin zone but treat each branch as one branch in the larger zone.

Soft-mode dispersion curves in FE are not available, but we have seen from the neutron data that the soft mode in PE beyond $\vec{Q}_M + \frac{1}{2}|Q_M|\hat{f}$ is not affected by the phase transition. If we assume that the same condition holds in FE also, then the same conditions which were used to specify the dispersion curves in PE can also be used in FE.

The bilinear coupling term ($\Delta\tilde{C}_{11}^L$) depends on the ratio of the soft-mode frequency Ω_η to the static value of the order parameter η_0. Since both Ω_η and η_0 decrease when the temperature is increased from

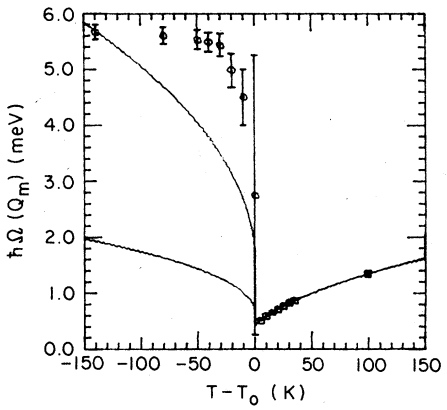

FIG. 5. Temperature dependence of the soft-mode frequency close to the phase transition. The data points are taken from the neutron experiments of Dorner *et al.*[23,24] Note that the data points in the range $T_0 \leq T \leq T_0 + 50$ K were derived from the neutron scattering cross section and not by direct measurement. The curve through the data points above T_0 indicates the results of the neutron scattering experiments. Below T_0, the lower curve shows the frequency of the "missing" soft-mode branch found from the model 3 fit to $\tilde{C}_{11}$ where its eigenvector is constrained to be parallel to the order parameter. The upper curve shows the frequency of the "missing" branch found with model 4 where the orientation of the two soft modes relative to the direction of the order parameter was not constrained and was found to be $\psi = 44 \pm 5°$.

room temperature towards the transition, their temperature dependences are largely canceled. The resulting magnitude of the bilinear anomaly varies from 0.76×10^{11} dyn/cm^2 at room temperature to 0.60×10^{11} dyn/cm^2 at the transition. Although the total predicted anomaly has about the right magnitude, it changes by only 0.1×10^{11} dyn/cm^2 between room temperature and the transition. This is much too small to account for the 1.3×10^{11} dyn/cm^2 change seen over the temperature range in the experimental data in Fig. 4.

There is another difficulty in assuming that the two branches of the soft mode are nearly degenerate. In deriving the elastic anomaly from the free energy in Sec. III, the soft-mode frequency below T_0 was found to depend on the free-energy parameters B and D through

$$m^* \Omega_\eta^2 = [2B + 4D\eta_0^2(T)]\eta_0^2(T) \quad . \tag{5.4}$$

The temperature dependence of Ω_η as derived from this equation would be much greater than that of the Fleury mode irrespective of the choice of the constants B and D, assuming that $\eta_0^2(T)$ follows Eq. (5.1).

We are thus led to conclude that the acoustic anomaly in FE cannot be explained if the two branches of the soft mode are nearly degenerate, since the bilinear term $\Delta\tilde{C}_{11}^L$ is nearly temperature independent while the fluctuation term $\Delta\tilde{C}_{11}^F$ is insignificant. Allowing η_0 to vary cannot improve the fit since it only displaces $\Delta\tilde{C}_{11}^L$ without increasing its temperature dependence. Some improvement can be obtained by simultaneously decreasing η_0 and increasing K_2, but the theory would then no longer fit the data in PE, nor would the observed temperature dependence of the order parameter $\eta_0^2(T)$ agree with Eq. (5.4).

Model 2 is suggested by the interpretation of Dorner *et al.* and corresponds to the last case in Fig. 9 of Ref. 24. It can be understood by examining the first three terms in the free energy [Eq. (3.16)] which give the complete dependence of G on η at constant strain. If the coefficients of the ϕ-dependent terms (B_2, B_3, D_2, and D_3) all vanish, then $G(\eta)$ is a figure of revolution. For $A < 0$ it becomes a "Mexican hat" so that the transverse mode is at zero frequency—the usual Goldstone mode which results when a continuous symmetry is broken. If some of these coefficients are nonzero but small, then the continuous symmetry is replaced by a discrete symmetry and $G(\eta)$ is a "bumpy Mexican hat" with four minima around the brim. The transverse frequency can still be very small, however, and constitutes a "pseudo-Goldstone mode." Note that $\Omega_\parallel$ and $\Omega_\perp$ can be very different even though the original tetragonal symmetry is only slightly broken. The effect of the low-frequency transverse mode in this model would be to increase the fluctuation integral relative to model 1, without changing the bilinear term. The temperature dependence of $\tilde{C}_{11}$ in *both* phases would then be primarily due to fluctuations.

Unfortunately, we cannot quantitatively compare our elastic constant data with the predictions of this model since no data for the transverse mode frequency and its dispersion are available. By arbitrarily adjusting the temperature dependence of its frequency we could probably find a good fit to $\tilde{C}_{11}(T)$. However, we would still be left with the second problem encountered in model 1: the order parameter is related to the *longitudinal* soft-mode frequency by Eq. (5.4), and the temperature dependence of the order parameter predicts a much stronger temperature-dependent $\Omega_\parallel(T)$ than that of the Fleury mode.

Model 3: In model 3, we assume that the Fleury mode is the *transverse* mode, and attempt to deduce the temperature dependence of the "missing" (longitudinal) mode. Although at variance with the eigenvector determination of Dorner *et al.* this model allows us to fit the elastic constant data and also to satisfy Eq. (5.4). We shall use $\delta\eta_1$ and Ω_1 to denote the dynamical variable and frequency of the "missing" soft-mode branch, and $\delta\eta_2$ and Ω_2 for the "Fleury" branch. Ω_1 will be treated as a free variable to be evaluated through fitting of the observed elastic anomaly. We continue to assume that the

eigenvectors of the two branches of the soft mode satisfy the condition $\delta\vec{\eta}_1 \| \vec{\eta}_0$; $\delta\vec{\eta}_2 \perp \vec{\eta}_0$ as we did in Sec. III.

The Fleury branch would produce no bilinear anomaly because now its eigenvector is perpendicular to the spontaneous displacement. Its contribution to the fluctuation anomaly is very small since its frequency is high, and can therefore be neglected. Thus we can analyze the elastic anomaly in FE as being due to the missing branch alone.

Equation (5.4) gives the soft-mode frequency in terms of the free energy parameters B and D. The number of parameters can be reduced by noting that at the transition, the spontaneous displacement $\eta_0^2(T_0)$ is

$$\eta_0^2(T_0) = -\frac{3(B - K_2^2/2\tilde{C}_{11}^0)}{4D} .$$

Using this equation, we may express Ω_η in terms of B alone:

$$m^*\Omega_\eta^2(T) = [2B - 3(B - K_2^2/2\tilde{C}_{11}^0)R(T)]\eta_0^2(T) .$$

$R(T)$ is given by Eq. (5.1) and is the ratio of the soft-mode amplitude at temperature T to its amplitude at the transition temperature T_0. The bilinear coupling $\Delta\tilde{C}_{11}^L$ which would be associated with this mode is then:

$$\Delta\tilde{C}_{11}^L = \frac{K_2^2}{[2B - 3(B - K_2^2/2\tilde{C}_{11}^0)R(T)]} .$$

Note that $\Delta\tilde{C}_{11}^L$ depends on the soft-mode amplitude relative to its value at the transition but not on its absolute magnitude. The functional dependence of $\Delta\tilde{C}_{11}^L$ can be made explicit by multiplying both numerator and denominator by $2\tilde{C}_{11}^0/K_2^2$. $\Delta\tilde{C}_{11}^L$ then becomes

$$\Delta\tilde{C}_{11}^L = \frac{2\tilde{C}_{11}^0}{[2\alpha - 3(\alpha - 1)R(T)]}, \quad \alpha = \frac{2B\tilde{C}_{11}^0}{K_2^2} . \tag{5.5}$$

In this form, one sees clearly that $\Delta\tilde{C}_{11}^L$ depends only on the relative size of B and $K_2^2/2\tilde{C}_{11}^0$ and its magnitude would be insensitive to the uncertainties in K_2 found from the data above the transition.

Due to the similarity in the curvature of $\tilde{C}_{11}$ in PE and FE, one might expect that $\Delta\tilde{C}_{11}^L$ should be relatively temperature independent with the curvature coming from the fluctuation term $\Delta\tilde{C}_{11}^F$. Therefore, it is of interest to examine the temperature dependence of $\Delta\tilde{C}_{11}^L$ as α is varied. The value of α must be such that $(\alpha - 1) < 0$ or $(B - K_2^2/2\tilde{C}_{11}^0) < 0$ because this combination of constants is the fourth-order coefficient of η_0 in the free-energy expansion which includes the effects of coupling and is negative in the case of a first-order phase transition. From Eq. (5.5), $\Delta\tilde{C}_{11}^L$ would be temperature independent if $\alpha = 1$. This corresponds to the limit when the transition is second order. In this case, $\Delta\tilde{C}_{11}^L = \tilde{C}_{11}^0$ and the predicted magnitude of the drop in $\tilde{C}_{11}$ is too large. As the value of α is reduced from 1, the magnitude of $\Delta\tilde{C}_{11}^L$ is also reduced. However, because $R(T)$ in TMO ranges from 1 at the transition to 4.5 at room temperature, the second term in the denominator of Eq. (5.5) quickly becomes dominant and $\Delta\tilde{C}_{11}^L$ depends on temperature as $1/R(T)$. In that case, $\Delta\tilde{C}_{11}^L$ would have more temperature dependence than is present in the experimental data. Clearly, there would have to be a tradeoff between the magnitude of $\Delta\tilde{C}_{11}^L$ and its curvature.

Thus far, we have carried out this discussion using a simplified free energy with one soft mode and one elastic strain. We have seen how the coupling to the strain can alter the temperature dependence of the uncoupled soft-mode amplitude. In reality, the true soft mode must include the influence of not one but all of the elastic constants. If this is done, the essential point of the preceding argument remains unaltered; however, in Eqs. (5.3) and (5.4) one should replace

$$(B - K_2^2/2\tilde{C}_{11}^0)$$

by

$$\left(B - \frac{K_2^2}{(\tilde{C}_{11}^0 + \tilde{C}_{12}^0)} - \frac{K_3^2\cos^2 2\phi_0}{2\tilde{C}_{66}^0}\right) .$$

The new equations for $\Delta\tilde{C}_{11}^L$ and Ω_1^2 are

$$\Delta\tilde{C}_{11}^L = \frac{2(\tilde{C}_{11}^0 + \tilde{C}_{12}^0)}{[2\alpha - 3(\alpha - 2 - \beta)R(T)]} , \tag{5.6a}$$

$$m^*\Omega_1^2 = \frac{K_2^2\eta_0^2(T_0)}{2(\tilde{C}_{11}^0 + \tilde{C}_{12}^0)}[2\alpha + 3(\alpha - 2 - \beta)]R(T) , \tag{5.6b}$$

where β is the ratio of $K_2^2\cos^2 2\phi_0/2\tilde{C}_{66}^0$ to $K_2^2/2(\tilde{C}_{11}^0 + \tilde{C}_{12}^0)$. The constraint on α now becomes

$$(\alpha - 2 - \beta) < 0 .$$

The fluctuation anomalies are given by Eq. (3.17). That of the Fleury mode is insignificant and is not included in the fitting.

The value of β is related to $\eta_0^2(T)$ and the shear angle $\tilde{\epsilon}_6(T)$ by

$$K_3\cos 2\phi_0\eta_0^2 = \left(\beta K_2^2\frac{\tilde{C}_{66}^0}{(\tilde{C}_{11}^0 + \tilde{C}_{12}^0)}\right)^{1/2}\eta_0^2(T)$$

$$= 2\tilde{C}_{66}^0\tilde{\epsilon}_6(T) . \tag{5.7}$$

The magnitude of η_0 and $\tilde{\epsilon}_6$ at room temperature (RT) were determined to be $\eta_0(\mathrm{RT}) = 1.65$ Å (Ref. 41) and $\tilde{\epsilon}_6(\mathrm{RT}) = 5$ min.[28] Using the value of β determined from Eq. (5.7) and adjusting α via Eq. (5.6a) to match the elastic anomaly at room temperature, we find $\Delta\tilde{C}_{11}$ to be too strongly temperature dependent and a satisfactory fit to the data is not pos-

sible. This is true even if K_2 is left as a free variable in view of its large uncertainty from the PE fit, and the data in PE and FE are analyzed simultaneously.

A better fit to the data is possible if α, β, and K_2 are all left as free variables when the data in PE and FE are analyzed. The resulting fit in FE is shown in Fig. 4. (The PE fit is not significantly altered from our earlier result.) The values for α, η_0 are (-2.84 ± 0.3) and (-0.53 ± 0.07) Å, respectively. K_2^2 and the other parameters are found to be quite insensitive to the data in FE and retain the values previously obtained. This result is evident from Eq. (5.6a) for the bilinear anomaly which forms the dominant part of the anomaly in FE and is dependent only on α and η_0. From Eq. (5.7), the corresponding value of η_0 is 0.53 ± 0.07 Å which is considerably below Jeitschko's measurement. The frequency Ω_1 of the missing branch is plotted in Fig. 5. Its frequency at room temperature is 2.3 meV. According to the Birman-Worlock theorem, the missing branch should be Raman active.[8] Neither the Raman scattering nor the neutron scattering experiments have revealed a feature in this frequency range, although it is at sufficiently low frequencies to possibly be obscured by strong elastic scattering, and might have a very small Raman strength.

Model 4: In analyzing the data in FE thus far, we have assumed that the eigenvector of one of the two soft modes is parallel to the spontaneous displacement. This assumption implies that the elastic anomaly is due to either the Fleury branch or the missing branch. We have found that neither alternative produces a satisfactory fit to the data without introducing properties of the soft mode which are inconsistent with the results of other experiments. In model 4 we therefore relax the condition that one of the soft-mode eigenvectors is parallel to the spontaneous displacement. From the discussion following Eq. (3.16), we see that if we set $(\delta\vec{\eta}_1 \cdot \vec{\eta}_0) = \cos\psi$ and $(\delta\vec{\eta}_2 \cdot \vec{\eta}_0) = \sin\psi$, the bilinear elastic anomaly is

$$\Delta\tilde{C}_{11}^{L} = \cos^2\psi \frac{K_2^2 \eta_0^2}{m^* \Omega_1'^2} + \sin^2\psi \frac{K_2^2 \eta_0^2}{m^* \Omega_2'^2} \quad , \tag{5.8}$$

where we now designate Ω_1' as the frequency of the missing branch. $\Omega_2'(T = 273\ \text{K})$ will be set equal to the Fleury branch frequency to be consistent with the results of Fleury, Petzelt, Kim and Ullman, and Shigenari *et al.*, while ψ and the temperature dependence of Ω_1' will be treated as free variables. Equation (5.6), which was derived from the free energy, is valid for a dynamical mode oscillating parallel to the spontaneous displacement. The expression for the soft-mode frequency is more complex in other directions. However, the *form* of the expression should be similar although the meaning of the parameters may be altered. We shall assume that Eq. (5.6b) continues to be valid for the temperature dependence of Ω_1' in the present case. We shall set $\eta_0 = 1.65$ Å in agreement with Jeitschko's results.

The bilinear anomaly due to the Fleury mode was seen to be only weakly temperature dependent. We shall therefore assume that it is a constant equal to its value at room temperature. The fluctuation anomaly of the Fleury mode is again neglected as insignificant.

We have carried out the data fitting under these assumptions and the results are shown in Fig. 6. The resulting values of the free parameters are

$$\tilde{C}_{11}^{0}(T) = [(8.07 \pm 0.1) - (0.000\,28 \pm 0.0003)(T - T_0)] \times 10^{11} \frac{\text{dyn}}{\text{cm}^2} ,$$

$$K_2^2 = (0.236 \pm 0.02) \times 10^{52} (\text{dyn/cm}^4)^2 ,$$

$$C_z = (16.8 \pm 1.0)\text{meV} ,$$

$$\cos^2\psi = 0.51 \pm 0.07 \quad (\psi = 44 \pm 5^\circ) .$$

Note that the error limits on K_2^2 and C_z are considerably reduced relative to the first fit. This is because the value of K_2^2 has now been adjusted to fit the experimental data at room temperature. However, the corresponding value of C_z shows that the dispersion in the $\hat{z}$ direction is much greater than in the xy plane.

The value of Ω_1 was derived via Eq. (5.6b) and is plotted in Fig. 5. Both Ω_1' and Ω_2' lie within the single broad feature observed in the Raman spectrum

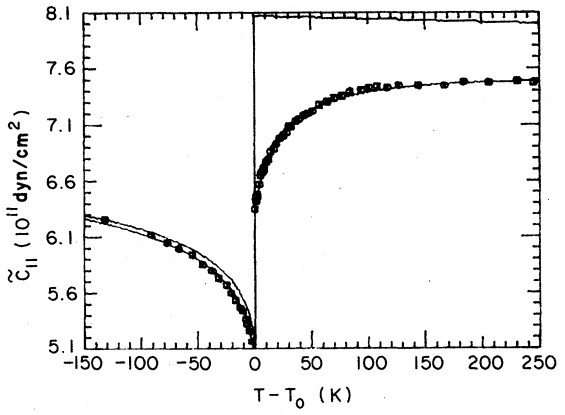

FIG. 6. Results of the fit of the $\tilde{C}_{11}$ data of TMO with model 4. The data were analyzed using a model in which the eigenvectors of the two soft modes were unconstrained and were found to be oriented at $\sim 45°$ to the direction of spontaneous displacement. As in Fig. 4, the upper curve above T_0 represents the background elastic constant in the absence of coupling while the lower curve includes the effects of critical fluctuations. The upper curve below T_0 represents the effects of induced bilinear coupling alone while the lower curve includes both bilinear coupling and the additional contribution from critical fluctuations.

between room temperature and T_0. Although Fleury's[30] analysis of this feature as a single mode suggested strongly temperature-dependent damping, the analysis of the Raman data by Shigenari *et al.*[33] in terms of two damped harmonic oscillators gave frequencies Ω_1 and Ω_2 closely resembling our present results up to approximately 100 °C. (They were unable to extend their two mode analysis closer to T_0.) The soft-mode frequency found here is also consistent with one alternative form of soft-mode splitting considered by Dorner *et al.* in the Appendix of their paper.

The rotation of the soft-mode eigenvectors relative to the orientation of the order parameter η_0 indicated by model 4 seems unreasonable at first glance but can be justified, at least conceptually, by consideration of the distinction between the high frequency and static free energies. If there were no coupling between η and the strain, the free energy associated with the order parameter would be given by the power-series expansion in η whose leading terms (in η^2, η^4, and η^6) are included in the first set of brackets in Eq. (3.15). In the low-symmetry phase where A is negative, $\vec{\eta}_0$ would lie in one of the four minima of the "bumpy Mexican hat." The eigenvectors of the two soft modes would be oriented in the directions of the maximum and minimum curvature of G at this point which, by symmetry, are parallel to and perpendicular to $\vec{\eta}_0$.

However, the equilibrium $\vec{\eta}_0$ is determined by the full free energy, including coupling to strains, which renormalizes some of the coefficients. In the simplified one-dimensional model discussed at the beginning of Sec. III, we saw that B, the coefficient of the quartic term in η in Eq. (3.1), appears as the renormalized coefficient $(B - K^2/2C)$ in Eq. (3.2a) which determines η_0. Similarly, in the equation preceding Eq. (5.6a) the renormalized version of B based on the full free energy is seen to contain a term which is dependent on ϕ. Thus the high-frequency ("clamped") and low-frequency or static free energy surfaces may be rotated with respect to each other.

The soft-mode dynamics are governed by the high-frequency free energy. Thus the equilibrium $\vec{\eta}_0$ which occurs at a minimum of the static free energy may not be at a minimum of the high-frequency free energy so that the orientation of the eigenvectors relative to $\vec{\eta}_0$ need not be parallel and perpendicular. This argument, though qualitative, may explain the surprising results of model 4.

We have also carried out a preliminary investigation of the elastic anomalies of C_{11} and C_{22} using the free-energy parameters determined from the fitting of $\tilde{C}_{11}$. So far, the resulting fit has been unsatisfactory. The main difficulty lies in the relatively small value of the ratio $K_3 \cos 2\phi / K_2$. From Eq. (3.19) (which is applicable at room temperature because of soft-mode degeneracy), one sees that the difference in the elastic behavior of C_{11} and C_{22} is the result of the coupling constant $K_3 \cos 2\phi_0$. The magnitude of $K_3 \cos 2\phi_0$ obtained from fitting of $\tilde{C}_{11}$ suggests that the difference between C_{11} and C_{22} should be much smaller than observed.

VI. CONCLUSIONS

We have investigated the anomalous elastic behavior of TMO and analyzed our results using a phenomenological model which includes both the effects of morphically induced bilinear coupling and of critical fluctuations. A self-consistent picture of the elastic anomaly both above and below the phase transition was obtained subject to the constraints of those soft-mode characteristics which are known from previous x-ray, Raman, infrared transmission, inelastic neutron scattering, birefringence, and thermal expansivity experiments.

Our results suggest that the nature of the two-dimensional soft mode in the ferroelectric phase is not yet well understood. We infer that the doubly degenerate soft mode in the paraelectric phase is split below the phase transition with the "missing" mode being strongly temperature dependent. Furthermore, because of the doubling of the unit cell, there are four branches of the soft mode below T_c. All four of these branches are of A_1 symmetry at the Γ point. The Fleury mode and the "missing" mode found in our analysis represent the two lowest branches of this soft-mode quartet. The high-frequency pair may correspond to the 75-cm^{-1} doublet reported by Kim and Ullman.[31] Our analysis has also produced specific predictions for the dispersion of the soft mode along the $\hat{z}$ axis which has not been determined by the neutron scattering experiments. In addition, the eigenvectors of the two soft modes below T_c in model 4 which gave the best fit to all the data were found to lie at approximately 45° to the direction of the spontaneous displacement (order parameter). We emphasize that this angle should be distinguished from the angle between the spontaneous displacement and the orthorhombic crystalline axes which has been the subject of considerable controversy.[24,39]

Our results imply a clear distinction between the physical origin of the elastic anomalies in the two phases. While the anomaly in the paraelectric phase is entirely due to coupling between the elastic strain $\tilde{\epsilon}_1$ and critical fluctuations of the soft mode, the effects of these fluctuations in the ferroelectric phase were found to be small compared to that of the morphically induced bilinear coupling. That these two effects can be calculated from the same wave-vector-independent coupling constant supports the validity of our phenomenological approach. We note that while critical fluctuations can, in general, lead to breakdown of the Landau free energy predictions, the

transition in TMO is first order by at least 4 K which effectively precludes such a possibility in this case. In fitting the data for the elastic anomaly, we have not taken the "adiabatic correction" into account since Toledano has shown that it is small for the rare-earth molybdates.[49] We point out that our analysis has only dealt with the elastic anomaly of $\tilde{C}_{11}$ for which the theory is relatively simple. Preliminary attempts at fitting the data for C_{11} and C_{22} using parameters derived from the fit to $\tilde{C}_{11}$ have not been successful. Fleury has suggested that the near degeneracy of the two soft-mode branches might lead to large additional contributions to the elastic anomaly from cross terms between the two soft-mode branches and the elastic strain. (These terms occur in C_{11} and C_{22}, but not in $\tilde{C}_{11}$.)

We recognize that some of the approximations built into our analysis, such as the assumed constancy of K_2 throughout the Brillouin zone and the truncation of the fluctuation corrections at the lowest order may well have influenced our numerical results. Finally, we note that the phenomenological theory makes specific prediction for the damping of the various elastic constants. Investigation of the acoustic damping as well as its pressure dependence could provide additional tests of the validity of the phenomenological theory.

ACKNOWLEDGMENTS

We wish to thank J. Barkley and L. Brixner of the Central Research Department, E. I. DuPont De Nemours and Company, and G. M. Loiacono of the Philips Laboratories for generously providing several excellent rare-earth molybdate crystals. We also thank Claude Ecolivet who participated in the instrumentation and programming of the spectrometer. We are indebted to J. C. Toledano, J. D. Axe, U. T. Hochli, P. Raccah, P. A. Fleury, J. Barkley, and W. A. Smith for numerous helpful discussions concerning the properties of these crystals. We are particularly grateful to A. P. Levanyuk for a most enlightening discussion of his theory of acoustic anomalies which has formed the basis of the analysis presented in this paper. This work was supported by the National Science Foundation under Grant No. DMR-77-23788 and by the PSC-BHE Research Award Program of CUNY.

---

*Present address: Perkin Elmer Corporation, Main St. Mail Sta. 283, Norwalk, Conn. 06856.

[1] *Structural Phase Transitions and Soft Modes,* edited by E. J. Samuelsen, E. Andersen, and J. Feder (Universitets Forlaget, Oslo, 1971).
[2] J. F. Scott, Rev. Mod. Phys. 46, 83 (1974).
[3] P. A. Fleury, J. Acoust. Soc. Am. 49, 1041 (1971), and references cited therein.
[4] V. L. Ginzburg, A. P. Levanyuk, and A. A. Sobyanin, Phys. Rep. 57, 151 (1980).
[5] E. M. Brody and H. Z. Cummins, Phys. Rev. Lett. 21, 1263 (1968).
[6] See R. L. Reese, I. J. Fritz, and H. Z. Cummins, Phys. Rev. B 7, 4165 (1973), and references therein for a discussion of the elastic anomaly where bilinear coupling is allowed.
[7] P. B. Miller and J. D. Axe, Phys. Rev. 163, 924 (1967).
[8] J. L. Birman, Phys. Lett. 45A, 196 (1973).
[9] J. C. Toledano, Ann. Telecommun. 29, 249 (1974); H. Z. Cummins, Philos. Trans. R. Soc. London Ser. A 293, 393 (1979).
[10] J. D. Axe and G. Shirane, Phys. Rev. B 1, 342 (1970).
[11] R. W. Gammon and H. Z. Cummins, Phys. Rev. Lett. 17, 193 (1966).
[12] See J. C. Slonczewski and H. Thomas, Phys. Rev. B 1, 3599 (1970); for a discussion of elastic anomalies in crystals in which linear coupling is forbidden.
[13] H. H. Barrett, Phys. Rev. 178, 743 (1969).
[14] G. Shirane and Y. Yamada, Phys. Rev. 177, 858 (1969).
[15] A. P. Levanyuk and D. G. Sannikov, Sov. Phys. Usp. 17, 199 (1974).
[16] P. A. Fleury and P. D. Lazay, Phys. Rev. Lett. 26, 1331 (1971).
[17] R. O. Bell and G. Rupprecht, Phys. Rev. 129, 90 (1963).
[18] B. Golding, Phys. Rev. Lett. 25, 1439 (1970).
[19] V. Dvorak, Phys. Rev. 167, 525 (1968).
[20] E. Pytte, Phys. Rev. B 1, 924 (1970).
[21] E. Pytte and J. Feder, Phys. Rev. 187, 1077 (1969); Phys. Rev. B 1, 4803 (1970).
[22] A. P. Levanyuk, Sov. Phys. JETP 22, 901 (1966).
[23] J. D. Axe, B. Dorner, and G. Shirane, Phys. Rev. Lett. 26, 519 (1971).
[24] B. Dorner, J. D. Axe, and G. Shirane, Phys. Rev. B 6, 1950 (1972).
[25] H. J. Borchardt and P. E. Bierstedt, Appl. Phys. Lett. 8, 50 (1966).
[26] H. J. Borchardt and P. E. Bierstedt, J. Appl. Phys. 38, 2057 (1967).
[27] L. E. Cross, A. Fouskova, and S. E. Cummins, Phys. Rev. Lett. 21, 812 (1968).
[28] S. E. Cummins, Ferroelectrics 1, 11 (1970).
[29] M. E. Lines and A. M. Glass, *Principles and Applications of Ferroelectrics and Related Materials* (Oxford University Press, New York, 1977), p. 355ff.
[30] P. A. Fleury, Solid State Commun. 8, 601 (1970).
[31] F. G. Ullman, B. J. Holden, B. N. Ganguly, and J. R. Hardy, Phys. Rev. B 8, 2991 (1973); B. N. Ganguly, F. G. Ullman, R. D. Kirby, and J. R. Hardy, *ibid.* 13, 1344 (1976); Q. Kim and F. G. Ullman, *ibid.* 18, 3579 (1978).
[32] J. Petzelt, Solid State Commun. 9, 1485 (1971).
[33] T. Shigenari, Y. Takagi, and Y. Wakabayashi, Solid State Commun. 18, 1271 (1976).
[34] R. Laiho, S. D. Prokhorova, I. G. Siny, E. G. Kuzminov, V. D. Mikvabia, and T. M. Polkhovskaya, Ferroelectrics 21, 339 (1978).
[35] I. G. Sinii, S. D. Prokhorova, E. G. Kuzminov, V. D. Mikvabia, and T. M. Polkhovskaya, Bull. Acad. Sci. USSR, Phys. Ser. 43, 93 (1979) [Izv. Akad. Nauk SSSR,

Ser. Fiz. 43, 1685 (1979)]; J. Phys. Soc. Jpn. Suppl. (in press).
[36]M. Nisar, J. Garland, and P. M. Raccah (unpublished).
[37]P. Fleury and K. Lyons (private communication).
[38]E. Pytte, Solid State Commun. 8, 2101 (1970).
[39]V. Dvorak, Phys. Status Solidi B 45, 147 (1971); 46, 413, 763 (1971).
[40]A. P. Levanyuk and D. G. Sannikov, Sov. Phys. Solid State 12, 2418 (1971).
[41]W. Jeitschko, Acta Crystallogr. Sect. B 28, 60 (1972).
[42]D. J. Epstein, W. V. Herrick, and R. F. Turek, Solid State Commun. 8, 1491 (1970).
[43]S. I. Chizhikov, N. G. Sorokin, B. I. Ostrovskii, and V. A. Meleshina, Sov. Phys. JETP Lett. 14, 336 (1971).
[44]B. A. Agishev, S. K. Esayan, V. V. Lemanov, and T. M. Polkhovskaya, Sov. Phys. Solid State 20, 2012 (1978); S. K. Esayan, B. D. Laikhtman, V. V. Lemanov, and N. Mamatkulov, *ibid.* 20, 1632 (1978).
[45]J. M. Courdille, R. Deroche, and J. Dumas, J. Phys. (Paris) 36, 891 (1975).
[46]U. T. Hochli, Phys. Rev. B 6, 1814 (1972).
[47]S. Itoh and T. Nakamura, Phys. Lett. 44A, 461 (1973).
[48]S. Itoh and T. Nakamura, Solid State Commun. 15, 195 (1974).
[49]J. C. Toledano, C. R. Acad. Sci. Ser. B 279, 569 (1974); M. Busch, J. C. Toledano, and J. Torres, Opt. Commun. 10, 273 (1974).
[50]Y. Luspin and G. Hauret, J. Phys. (Paris) Lett. 35, L193, (1974); Ferroelectrics 13, 347 (1976).
[51]Y. Luspin and G. Hauret, Phys. Status Solidi B 76, 551 (1976); Y. Luspin, thesis (Universite d'Orleans, 1976) (unpublished).
[52]D. G. Sannikov, Sov. Phys. Solid State 4, 1187 (1962).
[53]E. Pytte (in Ref. 1, p. 151).
[54]L. D. Landau and E. M. Lifschitz, *Statistical Physics* (Addison-Wesley, Reading, Mass., 1958), pp. 124, 444.
[55]M. Busch, thesis (Universite de Paris VI, 1974) (unpublished).
[56]Model 146MA-1000-F, Rosemount Inc., Minneapolis, Minn.
[57]Model SC121, Hotwatt Inc., Danvers, Mass.
[58]Model GA52P2, GA61P2, Fenwal Electronics, Farmingham, Mass.
[59]G. M. Loiacono, Philips Laboratories (private communications).
[60]Uniblitz Model DS 122, Vincent Associates, Rochester, N.Y.
[61]J. D. Axe suggests that the dispersion should be nearly isotropic (private communication).